Co-funded by the European Union

D3.1 Network Architecture and Gateway Specification

Project number	**101096021**
Project name	**Truly Sustainable Printed Electronics-based IoT Combining Optical and Radio Wireless Technologies**
Project acronym	**SUPERIOT**
Call	**HORIZON-JU-SNS-2022**
Deliverable No	**D3.1**
Deliverable Name	**Network Architecture and Gateway Specification**
Status	**Final**
Dissemination level	**Public**
Due date of deliverable	**2023-08-31 (M08)**
Actual submission date	**2023-08-30 (M08)**
Resubmission date	**2024-12-20 (M24)**
ork package	**WP3 "Network Architecture"**
Lead beneficiary	**UOULU**
Authors	Konstantin Mikhaylov (editor), UOULU Eduardo Almeida, INESC TEC Nuno Almeida, INESC TEC Junaid Bocus, U of Bristol Helder Fontes, INESC TEC Mohammad Khalili, UOULU Utku Kumbul, IMEC-NL Konstantin Mikhaylov, UOULU Tiago Ribeiro, INESC TEC Hazem Sallouha, KU Leuven Sérgio Silva, INESC TEC
Reviewers:	Khodr Hammoud, KU Leuven Hazem Sallouha, KU Leuven Henrik Sandberg, VTT

The SUPERIOT project has received funding from the Smart Networks and Services Joint Undertaking (SNS JU) under the European Union's Horizon Europe research and innovation programme under Grant Agreement No 101096021, including top-up funding by UK Research and Innovation (UKRI) under the UK government's Horizon Europe funding guarantee.

Executive Summary

This document establishes the basis for the further design and optimization of the SUPERIOT network and the individual functionalities to be supported by it. Departing from the requirements of the potential SUPERIOT application, specified by SUPERIOT WP1 and reported in deliverable D1.1, and the state-of-the-art analysis, the functionalities to be supported and provided by the SUPERIOT network are identified. The 1) wireless connectivity and 2) localization are found to be obligatory, while the 3) wireless energy transfer is considered a nice-to-have one. In this document, we discuss the state-of-the-art and the means for implementing each of these functionalities first standalone and then within an integrated solution. We converge to a five-tier network architecture topology composed of (a) the RIoT nodes, (b) the gateways/access points, (c) the embedded PCs, (d) a network switch(es), and (e) a central (cloud) server is proposed and discussed. Subsequently, the design of the gateways/access points and embedded PCs, including the hardware components, is detailed. The information about the state-of-the-art and details on how the SUPERIOT network will be designed constitute the key results of this deliverable. Following the request for revision and provided comments, the information about network simulations, energy budget and communication performance analysis, and wireless energy transfer integration in the gateways, as well as a discussion on alignment of the SUPERIOT network architecture and 6G SNS one has been appended to the document. The document will be used in the further work of WP3 and by all subtasks in WP3 and reveal the planned network architecture for other WPs of the project (especially WP2 and WP4). The discussion of the technical state-of-the-art and analysis of the application requirements provided in this document can also be helpful for WP1 in assessing the feasibility and potential of the different applications and/or demonstrations.

Table of contents

Editions

Version	Date	Modified by	Modification
0.1	2023-05-02	Konstantin Mikhaylov, UOULU	Initial draft from template v 2.0; draft table-of-contents & some sections
0.2	2023-08-13	Konstantin Mikhaylov, UOULU Mohammad Khalili, UOULU Hazem Sallouha, KU Leuven Utku Kumbul, IMEC-NL	The first full draft compiled.
0.3	2023-08-29	Konstantin Mikhaylov, UOULU Mohammad Khalili, UOULU	Addressing the comments from the internal review and other comments received; Appendix 1 added.
1.0	2023-08-30	Konstantin Mikhaylov, UOULU	Overall harmonization and cleaning prior to submission.
2.0	2024-12-20	Eduardo Almeida, INESC TEC Nuno Almeida, INESC TEC Helder Fontes, INESC TEC Junaid Bocus, U of Bristol Konstantin Mikhaylov, UOULU Hazem Sallouha, KU Leuven Sérgio Silva, INESC TEC Tiago Ribeiro, INESC TEC	Modifications addressing the request for revision. Sections 3.2.3.10, 5.4.3, 5.6, 6, and 7 added; text in other sections revisited.

1 Acronyms

3GPP	3rd Generation Partnership Project
AI	Artificial Intelligence
AOA	Angle of Arrival
AP	Access Point
ARM	Advanced RISC Machines
BBB	Beaglebone Black
BLE	Bluetooth Low Energy
CPU	Central Processing Unit
CSK	Color Shift Keying
DC	Direct Current
DF	Decode-and-Forward
E-ink	Electronic Ink
FD-PDOA	Frequency Domain Phase Difference of Arrival
GFSK	Gaussian Frequency-Shift Keying
GPIO	General Purpose Input-Output
GPS	Global Positioning System
I/O	Input/Output
IDE	Integrated Development Environment
IM/DD	Intensity Modulation and Direct Detection
IoT	Internet of Things
IPS	Indoor Positioning System
LED	Light Emitting Diode
LoS	Line-of-Sight
LTE	Long-Term Evolution
MAC	Media Access Control
MCDM	Multi-Criteria Decision-Making
MIMO	Multiple-Input and Multiple-Output

ML	Machine Learning
NFC	Near Field Communication
NOMA	Non-Orthogonal Multiple Access
NR	New Radio
OFDM	Orthogonal Frequency Division Multiplexing
OFDMA	Orthogonal Frequency Division Multiple Access
OOK	On-Off Keying
OPV	Organic Photovoltaic
OQPSK	Offset Quadrature Phase Shift Keying
PC	Personal Computer
PCB	Printed Circuit Board
PDOA	Phase Difference of Arrival
PHY	Physical layer (of the communication stack)
PLC	Power Line Communication
PPM	Pulse-Position Modulation
PRU	Programmable Real-time Unit
PV	Photovoltaic
PWM	Pulse Width Modulation
QoS	Quality of Service
RAM	Random Access Memory
RCS	Radar Cross Section
RF	Radio Frequency
RFID	Radio Frequency Identification
RIS	Reconfigurable Intelligent Surface
RISC	Reduced Instruction Set Computer
RIoT	Reconfigurable IoT
RSS	Received Signal Strength
RTOS	Real-Time Operating System

RX	Receiver
Si	Silicon
SD-PDOA	Spatial Domain Phase Difference of Arrival
SDN	Software-Defined Networking
SDR	Software-Defined Radio
SLIPT	Simultaneous Lightwave Information and Power Transfer
SoC	System-on-Chip
SSH	Secure Shell
SQL	Structured Query Language
TD-PDOA	Time Domain Phase Difference of Arrival
TDOA	Time Difference of Arrival
TOA	Time of Arrival
TOF	Time of Flight
TX	Transmitter
UART	Universal Asynchronous Receiver/Transmitter
UOWC	Underwater Optical Wireless Communications
USB	Universal Serial Bus
UWB	Ultra-Wideband
V2I	Vehicle-to-Infrastructure
VLC	Visible Light Communication
VLP	Visible Light Positioning
WMN	Wireless Mesh Network
WP	Work Package

2 Introduction

2.1 Motivation

The SUPERIOT project aims to develop and demonstrate the novel concept of truly sustainable IoT, where sustainability is approached holistically and supported by multimodality in different domains: wireless connectivity, energy harvesting (EH), and positioning. Though the sustainable and flexible implementation of the hardware, especially the node, is a corner stone for reaching this ambitious goal, it cannot do the job and is not sufficient alone. To ensure the overall efficiency and sustainability of the system, they have to be addressed comprehensively at the system level. Therefore, the current document creates the basis for efficient networking of SUPERIOT nodes, and at the same time, identifies and ensures support of the required functionalities. Note that since the work on the methodology of sustainability quantification is currently actively ongoing in SUPERIOT task 1.4, and the respective results are not yet available, the discussion of the sustainability aspect in this document is qualitative rather than quantitive.

2.2 Summary

Sustainability by design	
Multi-mode **communications**:	light- and radio-based wireless connectivity
Multi-mode energy **harvesting**:	light- and radio based
Multi-mode **positioning**:	light- and radio-based
Reconfigurability:	node and network
Sustainable implementation:	printed electronics technology (node)
Sustainable use:	smart energy harvesting and management

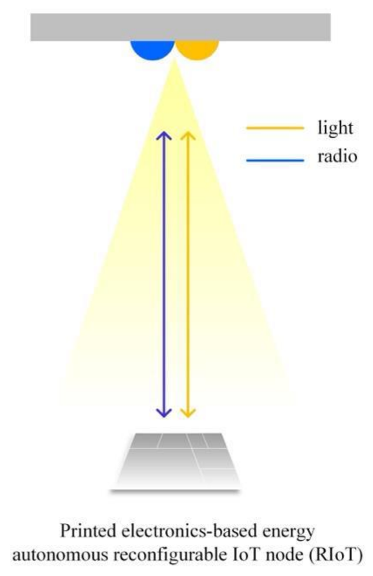

Figure 1: The key characteristics of the SUPERIOT concept [1].

Figure 1 reminds the key characteristics of the SUPERIOT concept. As discussed in [1], in the most simple case, a reconfigurable IoT (RIoT) node is connected to a single access point (AP) or a gateway[1], which provides optical (e.g., visible light communication (VLC)) and radio (i.e., radio frequency (RF)) based connectivity and other services (e.g., localization) to SUPERIOT end nodes[2] and/or high-level applications employing the nodes.

However, once we depart from this simplest scenario, some questions[3] arise, including:

- Where do the data go next from the AP?
- If there are multiple APs, how do they communicate between themselves?

[1] The terms access point and gateway are used interchangeably throughout the rest of this document.
[2] The details about the SUPERIOT node design are provided in SUPERIOT deliverable 2.1 entitled "Node architecture" [2].
[3] Note that the list presented is by no means comprehensive.

- Can all APs support both modalities (i.e., optical and radio) and offer all the desired functionalities (i.e., communication, localization, and EH)? Or are there more specialized APs (e.g., supporting only one optical/radio modality or just one functionality)?
- If multiple APs can serve a node, how to decide which APs serve it?

The current document addresses these and similar questions related to the SUPERIOT network architecture. We approach this challenge by first investigating the state-of-the-art, discussing the alternative implementation strategies and approaches for hybrid optical/radio networks, and then specifying the topology and elements of the SUPERIOT network, detailing the design of the key element of the SUPERIOT network infrastructure – the AP/gateway. The results presented in this document will be taken as inputs by the SUPERIOT work package (WP) 3 tasks and serve as the basis for interfacing the work done in WP3 with the other WPs (most notably WP2 and WP4). Note that the current document can also be revised throughout the project's lifetime to account for the recent research results and ensure state-of-the-art progress.

The current document has been prepared based on the discussions carried out received during a series of online meetings and the two face-to-face meetings (i.e., the kickoff meeting in Oulu, Finland, and the technical meeting in Aveiro, Portugal), a study of the state-of-the-art, and the offline work carried out by the partners.

2.3 Structure of the document

The structure of the remaining part of the document is as follows. We start by presenting the notation, identifying the network architecture components, and then discussing the relevant state-of-the-art in Section 3. Section 4 departs from SUPERIOT Deliverable 1.1 to analyse the pertinent requirements for network architecture design influenced by the potential SUPERIOT applications. In Section 5 we first detail the environment of operation and propagation media, then go through the architecture of communication, localization and energy transfer services. After that, we provide some highlights on integrating these services and reconfigurability and reusability aspects to be considered in the design. In Section 6 the initial results related to network simulations are presented. Furthermore Section 7 briefly revisits the 6G SNS architecture and discussed the alignment between 6G SNS architecture and SUPERIOT network architecture. In Section 8, we sketch the design of the SUPERIOT gateway. Following the same logic as in Section 5, we first discuss the communication, localization, and energy transfer services individually and how these functionalities can be integrated. Finally, Section 9 offers the conclusions and key results.

Note that Sections 3.2.3.10, 5.4.3, 5.6, 6, and 7 were introduced during the revision, addressing the comments and requests received. At the same time, modifications to other sections of the document were introduced.

3 Network architecture background

The current section offers a minimal background on network architecture and its key elements, as the SUPERIOT project understands them. Also, in the second subsection, we provide an overview of the related works relevant to multi-modal IoT.

3.1 Network architecture and other notations

In this document, we will use the following definition of network architecture originating from [3]:

"Network architecture serves as the comprehensive blueprint that outlines the structural layout and logical interactions within a network. This framework comprises hardware devices providing computation and communication capabilities, physical connections, and software applications orchestrating operational tasks. Further, it encompasses wireless networks, protocols that standardize the means of communication and data exchange, and an array of transmission media catering to diverse modalities of information transfer."

The network architecture can be further subdivided into four main components [4]:

- **Propagation Media**: This is the medium or media the network uses to transmit signals. The type of propagation media can significantly influence a network's performance, range, and reliability.
- **Network Topology**: Physical topology refers to the actual geometric layout of the elements, whereas logical topology refers to the path the data takes when moving from one point to another within the network. Network topology affects various aspects of a network, such as its resilience, latency, and cost-effectiveness.
- **Hardware and Software**: The tangible and virtual elements form the network's structure. Hardware includes all the physical devices, and software consists of any applications or approaches used to manage and direct the network.
- **Protocols**: These are the sets of rules that govern how data is transferred between network elements. Protocols define a common language and methodology that devices use to communicate with each other. They specify how signals should be formed, sent, received, and interpreted, ensuring that machines can understand each other and work together effectively.

3.2 State-of-the-art and related works

In recent years, the integration of optical communication with RF has garnered significant research interest, leading to the development of various approaches and techniques. The fundamental challenge lies in the seamless integration between optical and radio components, each with unique transmission characteristics and requirements. In this section, we present a review of the related work in optical/radio networks. We have categorized the related work into three areas: hardware components and propagation media, network topology, and software components and protocols. In the following, each category is individually presented and discussed.

3.2.1 Propagation media and hardware components

While hybrid optical-radio communications are predominantly explored in terrestrial applications, their potential extends to various indoor and outdoor settings. Inside buildings, the technology facilitates high-speed, low-latency communication networks that are ideal for offices, homes, and healthcare facilities. In supermarkets and retail environments, hybrid systems can support advanced inventory management systems and enable context-aware advertising through technologies like VLC. For outdoor applications, the technology shows significant promise in several areas, for instance, in smart cities, emergency services during disaster recovery, transportation systems, particularly in vehicular networks and Vehicle-to-Infrastructure (V2I) communications, and large outdoor events like concerts and sports gatherings. Further domains include precision agriculture, maritime operations at seaports or offshore installations, military deployments, and Industrial IoT setups.

Moving beyond traditional terrestrial applications, hybrid optical-radio communication systems have begun making inroads into more specialized domains. Underwater environments, for instance, can benefit from the approach to address the inherent limitations of Underwater Optical Wireless Communications (UOWC), like short-range and high signal attenuation. In such scenarios, optical systems excel at high-data-rate transmission over shorter distances, while RF serves as a more reliable medium for longer-range, albeit slower, communications.

In the realm of Space applications, laser-based optical systems offer advantages in terms of high data throughput over significant interstellar distances. On the other hand, RF systems continue to provide the robustness needed for command-and-control signals in inter-satellite networks. Commercial space stations are another frontier where optical communication can meet the demands of high data rates for tasks such as scientific experiments and video conferencing. RF is the go-to medium for routine operational tasks.

The essential hardware components of optical/radio networks typically encompass transmitters (TXs) and receivers (RXs) to support the required optical or radio interface functionalities. Optical TXs utilize light-emitting diodes (LEDs), infrared, or laser diodes to transmit data, dynamically altering light intensity within the spectrum range of 400 to 800 THz. Optical communication enables high-speed, secure, and energy-efficient communication; however, it remains susceptible to disruptions caused by ambient light interference and physical obstructions. In optical communication, intensity modulation, and direct detection (IM/DD) methods are employed with various modulation techniques to achieve optimal outcomes [5]. A range of modulation schemes has been proposed for optical communication, spanning through On-Off Keying (OOK), Pulse Width Modulation (PWM), Pulse-Position Modulation (PPM), Color Shift Keying (CSK), Orthogonal Frequency Division Multiplexing (OFDM), and others. Each scheme has distinct advantages and limitations, and the selection depends on precise application prerequisites and environmental factors such as data rate requirements, power efficiency, complexity, and specific usage scenarios [6]. On the other hand, RF communication utilizes distinct parts of the RF spectrum (3 kHz to 300 GHz), depending on the specific technology (e.g., Wi-Fi, cellular, Bluetooth). RF TXs generate electromagnetic waves sent through antennas and received by RF RXs. RF offers broader coverage and, depending on the frequency band, is suitable for non-line-of-sight (non-LoS) situations. Still, it may suffer from interference and has more rigorous licensing regulations [7].

The goal of integrating optical and RF communication is to capitalize on the individual strengths of both while mitigating their limitations. However, complex switching requirements between optical and radio modes can influence the system’s power consumption, data rate, transmission range, etc. Note that in optical/radio networks, optical and radio interfaces can operate concurrently or switch based on network conditions, user requirements, and Quality of Service (QoS) parameters [8]. Several research projects have been dedicated to exploring new modulation techniques for optical/radio devices. In [9], a hybrid OFDM methodology was introduced to integrate VLC and RF channels at the physical layer (PHY). This innovative OFDM approach enhances the allocation and optimization of power and bandwidth, facilitating superior network performance. Additionally, various research projects have endorsed using non-orthogonal multiple access (NOMA), which exhibits greater resilience to LoS interruptions than Orthogonal Frequency Division Multiple Access (OFDMA) [10]. NOMA can cause users to compete for resources; therefore, some studies suggest using a game strategy instead of a more common opportunistic method.

Integration of optical/radio networks with other technologies like Power Line Communication (PLC) can improve coverage and connectivity. One approach is to use optical/radio network for short-range communication while utilizing PLC as a reliable backbone for interconnecting APs and extending network coverage. Similarly, an infrared control channel was also implemented on the uplink of some optical/radio networks to transmit acknowledgement signals for optical data packets [11]. In addition, Reconfigurable Intelligent Surface (RIS) has been used for RF and gradually introduced into optical communication [12][13]. RIS is a metamaterial surface consisting of plenty of passive reflection surfaces, which can reconfigure the propagation environment. Therefore, some researchers introduced RIS for optical/radio networks [14]. Furthermore, variants of multiple-input and multiple-output (MIMO) methods, such as cell-free massive MIMO systems, have been proposed to improve the efficiency of optical and RF networks independently. Also, there are some efforts to use MIMO in hybrid optical/radio networks [8], [15], [16].

Meanwhile, certain research endeavours have been focused on integrating EH capabilities into hardware components, aiming to enhance the overall energy efficiency of optical/radio networks. For instance, simultaneous lightwave information and power transfer (SLIPT) have also been investigated in hybrid VLC/RF systems [16]. In [17], the researchers investigated a dual-hop hybrid VLC/RF communication system. The relay within this system harvested energy from the first-hop optical link by extracting the direct current (DC) component from the received signal. The harvested energy was then deployed to facilitate the transmission to the ultimate destination in the second-hop RF link. In [18], the authors evaluated the outage performance of a hybrid VLC/RF system that applied SLIPT in the downlink. The harvested energy from this process was then used to broadcast an RF signal in the uplink as a response. In [19], a hybrid VLC/RF system was analyzed where two separate TXs communicated with their respective RXs through a shared relay. This relay could harvest optical energy from the VLC system and carry out Decode-and-Forward (DF) relaying via an RF link to the RX.

3.2.2 Network topology

Network topology refers to the arrangement and connections between devices within a network. It can affect the interactions between technologies, signal interferences, transmission rate, performance, reliability, and adaptability. In real-world scenarios of optical/radio networks, topology defines the links between end devices, optical, and RF APs. In practice, most available research projects control the network topology by assigning the network devices to the optical, and RF APs, and topology control in the context of device-to-device communication within optical/radio networks remains a focus for only a limited number of studies [20], [21]. In cases where device-to-device communication is not incorporated into an optical/radio network configuration, the AP assignment defines the system's network topology. However, in scenarios where device-to-device communication is not considered, AP assignment only specifies a portion of the network topology of optical/radio networks. This subsection explores the seminal studies in AP assignment.

An individual node in the optical/radio network can be configured into five distinct operating modes based on the chosen optical and radio interfaces. These modes are as follows:

- Mode 1: fully optical;
- Mode 2: optical/radio for downlink/uplink, respectively;
- Mode 3: radio/optical for downlink/uplink, respectively;
- Mode 4: fully radio;
- Mode 5: simultaneous utilization of both optical and radio links.

The suitable mode can be selected through an algorithm that considers various input parameters [7]. Various factors, including security concerns, user and application requirements, physical medium conditions, user/operator decisions, and local operating policies, are considered when deciding whether to use optical or radio.

The number of alternatives in AP assignment in an optical/radio network is related to the number of optical APs, denoted by N_V, the number of RF APs, denoted by N_R, and the total number of network nodes, denoted by N_I. To consider both uplink and downlink connections for every node, the maximum number of potential alternatives in AP assignment in an optical/radio network is equal to $(N_V + N_R)^{2N_I}$. This expression represents the vast array of network configurations, accounting for the interplay between AP assignment, network topology, and the presence of other network nodes. It is essential to consider that wireless nodes' constrained transmission range and power might limit the potential associations with specific APs. Consequently, the formulated equation establishes the upper boundary for feasible scenarios within an optical/radio network context.

Current approaches in the assignment of one or multiple APs serving a node in optical/radio networks can be segmented into three main categories: heuristic algorithms, optimization frameworks, and machine learning (ML) approaches. Heuristic algorithms simplify decision-making by considering relevant factors and disregarding less significant details in AP assignments. For instance, Ghosh et al. in [22] utilized VLC links for high data rate applications and RF communication for wide area coverage with high reliability. These methods offer practical and efficient solutions for optical/radio networks, although they may not always ensure optimal outcomes. Optimization models formulate the problem of AP assignment in optical/radio networks as a mathematical optimization programming to find the best solution that optimizes a defined objective function while satisfying constraints. For instance, Wang et al. in [23] proposed joint lamp arrangement and power allocation algorithms to achieve uniform illumination and maximize achievable rates. Such models aim to find globally optimal solutions, ensuring optimal AP assignment based on the defined objective function and improving efficiency. However, scalability can be a concern when dealing with large-scale systems with numerous APs and devices. ML approaches have gained attention in optical/radio networks, offering adaptability, scalability, and the potential for self-optimization. They can predict network conditions and user demands, enabling proactive and intelligent network operations. They can also process and analyze large volumes of network data, generating valuable insights for network planning and optimization. For example, Kong et al. in [24] utilized multi-agent Q-learning to develop an online power allocation algorithm for mobile multi-homing users in hybrid VLC/RF networks.

As network topologies must adapt to dynamic network changes, less complex algorithms are often preferred for AP assignment in optical/radio networks. Network reliability, mobility, and handover factors are vital in determining AP assignment strategies. Moreover, network topology significantly influences various aspects of optical/radio networks, including load balancing, interference management, and resource allocation. These considerations are essential in the topology control of optical/radio networks. The upcoming subsection delves deeper into these concerns.

3.2.3 Software Components and Protocols

Software components and protocols are vital in managing and controlling optical/radio networks. They govern the encoding, decoding, modulation, and demodulation of signals and control the transmission and reception of data across the network. Networking protocols determine the structuring of data packets, their transmission and reception, as well as how errors are detected and corrected, ensuring efficient data transmission, error control, network synchronization, and resource allocation.

IEEE 802.15.7 standard provides the PHY and medium access control (MAC) layer protocols for VLC. These protocols tackle unique VLC system challenges, such as inter-symbol interference, multipath propagation, and shadowing [25]. Given their long history and widespread use, the RF protocols are more mature and diverse. For instance, the IEEE 802.11 family of standards provides the PHY and MAC layer protocols for Wi-Fi, incorporating various modulation schemes, MAC methods, and QoS mechanisms. Cellular technologies like Long-Term Evolution (LTE) and 5G New Radio (NR) have their protocols defined by the 3rd Generation Partnership Project (3GPP), covering a wide range of aspects from frequency bands and data rates to multiple access and network architecture.

In optical/radio networks, the protocols of both systems should work cohesively for efficient and reliable communication. Due to the distinctive characteristics of optical and radio networks, ensuring their seamless interoperation is a complex task, which makes proposing protocols for optical/radio networks more complex. Although there are no standard protocols for optical/radio networks, researchers have provided some relevant results on the following aspects:

3.2.3.1 Handover management

Ensuring a smooth transition between optical and radio interfaces is crucial for maintaining high-quality communication. Some factors, such as signal strength, network conditions, user mobility, and QoS requirements, influence this process. When making handover decisions, certain mechanisms are considered as additional elements such as location information, link quality, and network congestion. In [26], a versatile handover cost model was introduced to tackle the cost assessment challenge in hybrid VLC/RF networks. This model enables evaluation of the cost involved in various handover scenarios, considering different network setups and user mobility profiles. It provides a benchmark for assessing the performance of handover strategies, using metrics like handover overhead and rate, throughput, data rate, latency, and packet loss rate. In [27], the authors developed a location-based vertical handover technique. They discovered increased light path obstructions with a growing number of users, leading to performance degradation. In [28], an event-driven adaptive handover mechanism was proposed for centralized hybrid VLC/millimetre-wave systems. This mechanism employs offset-enhanced signal-to-interference plus noise ratio levels of APs as performance indicators.

3.2.3.2 Energy Efficiency

Energy efficiency is paramount in sustainable systems like optical/radio networks underlying the SUPERIOT concept. The efficient functioning of these systems necessitates optimizing power consumption for both optical and RF interfaces alongside strategic, operational management. Importantly, optical communication, which is commonly integrated with lighting fixtures, can modulate light, thus not requiring additional energy consumption. In the case if light-based communication is deployed standalone, several strategies enhance energy conservation in optical communication. For instance, dimming control allows for brightness adjustment of LEDs based on illumination and data transmission needs. In optical/radio networks, coordinating the operation of optical and RF interfaces is a practical approach to improve energy efficiency. Actions may include selecting the most energy-efficient interface for data transmission, dynamically switching between optical and RF interfaces based on their energy consumption and communication performance, and implementing load balancing to distribute data traffic and minimize power usage evenly. The energy efficiency of optical/radio networks can be further improved with advanced technologies like EH, adaptive modulation, sleep mode management (stop operation of transceivers during periods of inactivity), power control (adjust transmission power in response to signal quality and interference levels), massive MIMO and beamforming (direct transmission power towards desired areas). This is worth noting that optimising the energy efficiency at a system level, including selecting the subset of active components, is crucial for attaining high overall sustainability of the SUPERIOT system.

3.2.3.3 Resource allocation

The resources (e.g., power, bandwidth, battery) of many IoT systems, with the optical/radio networks considered by SUPERIOT not being an exception, are usually limited and efficient utilization of them is crucial for maximizing the overall performance and sustainability. These resources should be distributed among users to achieve certain optimization goals. Recent studies focus on maximizing throughput while minimizing power consumption, extending battery life, and ensuring sustainable operations. The dynamic and adaptive nature of these allocations, especially in environments with changing user requirements and external interferences, remains an area of active investigation. Due to the complexity of some approaches in resource allocation in optical/radio networks, some researchers employed cloud computing.

3.2.3.4 MAC layer

A major challenge for MAC in optical/radio networks is managing uplink (from user to network) and downlink (from network to user) transmissions across optical and RF mediums. The distinct nature of these links, combined with the disparate properties of optical and RF, makes collision avoidance and management especially critical. Several studies have probed into developing collision-free MAC protocols, exploiting VLC’s high-speed capabilities while leveraging RF’s reliability. Moreover, as the hybrid network evolves, ensuring balanced load distribution between uplinks and downlinks without compromising on throughput remains an active area of exploration. In [29], researchers introduced a MAC protocol tailored for hybrid VLC/RF systems to reduce network delay, energy usage, and collisions while boosting throughput. In [30], an advanced model was presented for simultaneous power and slot allocation in hybrid VLC/RF networks, targeting maximising the cumulative rate in downlink communication. They should provide fairness and user satisfaction. In [31], researchers leveraged MAC strategies to optimize the total data rate, making collective decisions on power allocation coefficients, pairing indices, and link choices.

3.2.3.5 Security and Privacy

Due to the LoS nature of light propagation and confined coverage of optical communication, it naturally prevents eavesdropping and unauthorized access, giving it inherent security advantages. However, its susceptibility to optical jamming and PHY attacks, such as signal interception and modification, poses challenges. Security methods like light encryption, secure channel coding, and PHY security approaches have been proposed to counter these. On the other hand, RF is prone to several types of attacks, including jamming, interception, and man-in-the-middle attacks. Conventional security mechanisms for RF encompass encryption, authentication, and intrusion detection systems. The security of RF can be enhanced by more advanced techniques, such as secure coding, dynamic spectrum access, and cooperative relaying. In optical/radio networks, the coordination between optical and RF interfaces can enhance security. For example, a secure handover between VLC and RF can be implemented to prevent potential attacks during the transition. Moreover, a multi-layer security scheme can be employed for comprehensive protection, utilizing VLC for secure data transmission and RF for secure control signalling or otherwise around. Privacy in optical/radio networks revolves around safeguarding user identity and sensitive data from unauthorized access and leakage. Techniques for privacy protection may include anonymization, pseudonymization, and secure multi-party computation. Ongoing research in optical/radio networks aims to develop efficient security and privacy solutions for hybrid and to incorporate these solutions into the network’s architecture and operation. This endeavour involves not only technical strategies but also regulatory and policy considerations. Blockchain technology can fortify the security, transparency, and trustworthiness of optical/radio networks. For instance, it can securely record and verify network transactions, such as data transmission and service usage.

3.2.3.6 Load balancing

To effectively capitalize on the strengths of both optical communications, with its high bandwidth and security, and RF, known for mobility support and extensive coverage, load balancing is essential. By adopting a user-centric approach to load balancing, users' unique preferences, including latency tolerance and application needs, can be addressed, ensuring optimal optical/radio network traffic distribution. It is crucial that this balancing strategy seamlessly integrates the interplay between optical and RF networks, considering handover mechanisms. Adept load balancing is key to optimizing resource utilization and guaranteeing superior communication quality in these hybrid systems.

3.2.3.7 Positioning

Visible light positioning (VLP), characterized by high accuracy, low power consumption, cost-effectiveness, and eco-friendliness, has gained substantial attention in positioning applications. Positioning in optical/radio networks leverages the strengths of both technologies. This precision is valuable for fine-tuned localization tasks. For instance, a two-step method can be employed in optical/radio networks where RF is utilized for coarse positioning because of its wider coverage. Then VLP steps in to refine and achieve higher positional accuracy. In addition, integrating optical and RF data can significantly enhance the precision of Simultaneous Localization and Mapping (SLAM) algorithms, making them more reliable in mixed environments. Furthermore, the environment can be mapped or “fingerprinted” based on signal strengths or characteristics from both optical and RF TXs. The position is later determined by comparing real-time measurements against this stored data.

3.2.3.8 QoS handling

Foundational QoS metrics such as latency, jitter, throughput, and packet loss rate are also important in optical/radio networks. Some studies have comprehensively analysed latency and throughput in optical/radio networks. They highlighted potential bottlenecks in hybrid configurations and proposed solutions to ensure optimal QoS. In addition, researchers introduced QoS-aware approaches for load balancing, resource allocation, and MAC layer tailored for optical/radio networks to provide the required QoS, reducing packet loss and improving overall system reliability. Furthermore, researchers developed some QoS optimization frameworks that considered the variable conditions of optical and RF channels and maintained QoS under varying environmental and network conditions.

3.2.3.9 Heterogeneous and multi-criteria nature

Optical/radio networks inherently exhibit heterogeneous characteristics. Consequently, any effective strategy targeting these networks should recognize and adapt to this nature while addressing the diverse applications and user requirements. Recognizing these refinements, researchers have developed specialized algorithms tailored to the unique requirements of optical/radio networks. Moreover, several attributes should be of concern to overcome issues of optical/radio networks; therefore, researchers could leverage Multi-Criteria Decision-Making (MCDM) methods in such systems. Note that MCDM offers a framework to balance various competing objectives, such as maximizing data rates, reducing latency, and ensuring equitable resource distribution within optical/radio networks. In parallel, Software-Defined Networking (SDN) presents an innovative approach to network management. SDN facilitates dynamic network adjustments, optimal resource distribution, and agile load balancing within optical/radio networks by decoupling the control plane from the data plane.

3.2.3.10 Energy harvesting, wireless power transfer, SWIPT and SLIPT

Reliable provision of energy to the IoT devices was identified as one of the corner requirements for the future energy-sustainable IoT ecosystem [32]. Compared to conventional ambient EH, wireless energy transfer (also known as wireless power transfer) denotes the intentional transmission of energy using dedicated transceivers to power IoT devices. Compared to ambient EH, wireless power transfer provides a more predictable and controllable means to power IoT devices [32]. Notably, when merged with communications (i.e., information transfer), the concept of simultaneous information and power transfer emerges; depending on the type of the signal used, two main brunches are identified – SWIPT and SLIPT for RF and light-based power transfer.

A survey of the SWIPT concept and recent results, especially in SWIPT application to the 5G technology, is provided in [33]. The paper surveys the multiuser SWIPT, including system design, applications, technical solutions and experimental results. Previous studies have explored SWIPT using various modulation techniques. Multisine waveforms have been used for dual-purpose energy transfer and information transmission, enhancing efficiency through optimizing peak-to-average power ratios (PAPR), as discussed in [34]. To mitigate information distortion in SWIPT, the biased amplitude-shift keying (ASK) and phase modulation waveforms were developed, as described in [35], respectively. A recent study, referenced in [36], introduces a multitone phase shift keying (PSK) modulation approach. This method demonstrates a reduction in voltage ripple at the diode output compared with ASK. Contrary to the amplitude variation-based modulation schemes (PSK and ASK) for SWIPT, the multitone frequency-shift keying (FSK) schemes presented in [37] have a lesser impact on wireless power transfer (WPT) performance. Though SWIPT is typically based on specially designed radio waveforms [38], the possibility of harvesting energy from BLE packets (thus implementing SWIPT) was conceptualised and demonstrated by the authors of [39]. Also relevant to the SUPERIOT work is the use of RIS in the context of SWIPT [40].

An overview of recent progress related to SLIPT is provided, e.g., in [41]. Compared to RF-based SWIPT, SLIPT can offer very high data rates, but is affected by ambient and sources, and features limited support for mobility and NLOS communication. The design guidelines, transceiver architectures as well as achievable data rates and limitations are discussed in the paper. The SLIPT is considered to be especially prospective for indoor applications[42] and underwater operations [43]. The integration and optimisation of SLIPT and RF has been looked at in, e.g., [44][45]. In the domain of zero-power SLIPT IoT sensors, research has highlighted the complexity of powering the IoT node while maintaining an optimal data rate, leading to a tradeoff between data rate and power harvesting, as detailed in [46]. This trend continues in studies like [47], [48], where either power harvesting or data transmission is the focus. Nevertheless, employing modulated light for data communication results in an unavoidable power penalty at the transmitter [49], due to the current-voltage convexity of the light-emitting diode (LED).

4 SUPERIOT requirements analysis for network architecture

Reference [1] offers an in-depth discussion of the key SUPERIOT technology features, most potential scenarios and applications for its utilization, and their requirements. Departing from the application requirements categories listed in that document, in Table 1, we map the identified application requirements against the elements of network architecture specified in the previous chapter. Note that for the sake of conciseness, we have grouped some related from the network architecture point of view requirements (e.g.," eco-friendly" and" sustainability" or" reconfigurability" and" reusability") together.

Table 1. SUPERIOT application requirements identified in [1] and the elements of network architecture affecting them.

Application requirements from SUPERIOT D1.1 [1]	Network architecture elements			
	Propagation media	Network topology	Hardware and software	Protocols
Communication/connectivity performance	v	v	v	v
Energy autonomy[4]	v	v	v	v
Positioning	v	v	v	v
Reconfigurability and reusability		v	v	v
Sensing & actuation			v	
Sustainable and eco-friendly manufacturing			v	
Specific form factor			v	
Cost-efficient manufacturing			v	

As one can see from Table 1, when we consider network architecture, all four of its elements will affect communication/connectivity performance, energy autonomy, and position. Furthermore, the three elements – network topology, hardware and software, and protocols also affect reconfigurability and reusability. The other application requirements, focusing on functionalities, sustainability, form factor, and manufacturing costs, are primarily affected by hardware and software design and implementation, not other network architecture elements.

Departing from this and considering that the functions of

- transferring the data (i.e., communication/connectivity),
- collecting and transferring the energy (i.e., energy autonomy),
- and positioning,

despite having some overlaps, are substantially independent. In the following section, we discuss the respective functional network architecture(s) separately and independently. Also, we offer

[4] We consider energy autonomy as a combination of energy harvesting and wireless power transfer techniques and optimization techniques at the device and network level focused on energy consumption minimisation.

some discussion on how these various architectures can be seamlessly integrated and reconfigurability/reusability aspects.

5 Functional network architecture(s)

We start this section by discussing the communication media, which is a common point for all three functionalities identified in the previous chapter. Then we proceed by examining each of the three functional architectures – for communication, localization, and energy transfer – in a dedicated subsection. Finally, in the two last subsections, we discuss the integration of the three functional architectures and reconfigurability/reusability aspects.

5.1 Propagation media

Except for the applications 3.3 (i.e., "Underwater IoT") and, partially, 3.4[5] ("In-body and on-body communication") and 3.6 (i.e., "Resource extraction supported by IoT communication"), all other potential SUPERIOT applications discussed in [1] imply at least part of the communication to happen through the air channel. The information about the wireless media and operation environment for the different applications is summarised in Table 2.

Table 2. Wireless media for SUPERIOT application identified in [1].

Application ID(s)[6] in [1]	Wireless media(s) and environment
1.1,1.2,1.6,1.11, 2.4,3.5,3.7	air (home/office/shop/street)
1.3	air (home/office/shop/street) + inside product (pill/food/package)
1.4,1.5,1.9	air (industrial)
1.7,1.9,2.3	air (hospital)
1.8,1.10	air (home/office/shop/street) + next to/inside body
2.1,2.2	air (home/office/shop/street) + inside walls
2.5	air (rural/forest)
3.7	air (streets/tunnels)

From Table 2 can be seen that in most cases, the distances of operation will be relatively short, with the only exception being application 2.5. At the same time, in most of the applications, one can expect that at some phases of operation, some devices might experience direct LoS and some non-LoS propagation due to shadowing and signal blockage. The latter suggests avoiding using mmWave RF signals, which are prone to substantial attenuation in materials. This can also be noted that most of the applications considered do not imply high-speed mobility and substantial change of the operation environment, though hardly one can expect that either of the environments would remain completely static and unchanged throughout the whole operation time of an application. For instance, most of the applications imply the presence of humans and/or vehicles in the area of operation, who can temporarily block the LoS.

All in all, this can be concluded that for most of the applications, the VLC and RF signals will propagate through the air, which is quite a convenient propagation medium for both optical and RF signals. Also, it can be seen that, in most cases, the signals will propagate indoors, possibly in the areas where other devices and systems are operating. This suggests the possibility of

[5] Note, that the demonstration of both applications 3.3 and 3.4 is considered in [1] to be out of the SUPERIOT project scope.
[6] For the sake of convenience and self-sufficiency, the list of scenarios and applications identified in [1] is provided in Appendix 1.

interferences from external systems (predominantly radio, optical communication and lighting, and other-purpose systems), which must be considered. Additionally, for the specific propagation environments and scenarios, the following needs to be considered concerning RF propagation:

- industrial and similar propagation environments: heavy multipath fading with good coverage behind obstacles and slow power attenuation for radio frequencies [50].
- hospital propagation environment: variation of the radio wave propagation characteristics from room to room (patient wards, operating rooms, X-ray and magnetic resonance tomography) [51].
- inter-vehicle communication: effect of the vehicle body [52] and, e.g., the difference in fading between open roads and tunnels [53].
- interference from third-party systems and devices (including, e.g., user smartphones) [54] in environments with high device density (e.g., streets, offices).
- and safety-related restrictions on the use of RF-based communication in particular environments (e.g., medical facilities and security areas).

Similarly, concerning the propagation of the optical signals, the following has to be considered:

- the potential of interference from the ambient light sources to the VLC systems [55],
- and restrictions on the use of RF-based communication in particular environments.

Notably, application 3.5 suggests the possibility of using RIS to extend the coverage. A RIS introduces a new level of flexibility by controlling and affecting the propagation channel [56]. However, this requires efficient mechanisms for controlling the RIS and its resources and finding the best configuration.

5.2 Network architecture for communication service(s)

Efficient connectivity is the critical functionality to be provided by the SUPERIOT network. The current section focuses on the connectivity requirements dictated by the identified potential applications and how they can be satisfied.

5.2.1 Application requirements analysis

In the following, we highlight the high-level requirements of sample applications from the three main scenarios considered in the SUPERIOT project. In particular, from a connectivity perspective, we define the following requirements [1]:

5.2.1.1 Scenario 1: Smart Tags

The smart tags scenario covers items that use smart tags/labels in supermarkets, items in hospitals, or animals in farm applications. The general requirements are:

- Data rate **low**,
- Coverage **medium** within a farm/supermarket/hospital,
- Energy efficiency **high**,
- Positioning **medium**.

5.2.1.2 Scenario 2: Large-scale IoT

Large-scale IoT applications are related to smart hospitals, smart buildings (indoor), and farming agriculture (outdoor). The general requirements are:

- Data rate **medium**; maybe QoS,
- Coverage **high**,
- Energy efficiency **high**,

- Positioning **high**.

5.2.1.3 Scenario 3: Demanding environments:

Examples of demanding environments are underwater and in-body IoT, where secure, private, and reliable IoT connections are crucial. The general requirements are:

- Data rate **medium**,
- Coverage **medium**,
- Energy-efficiency **high**,
- The positioning also varies based on the application, **medium/high**.

5.2.2 State-of-the-art

Most IoT networks adopt an uncoordinated star network architecture [57]. However, as the spatial density of IoT devices increases, the deployment of uncoordinated star networks becomes increasingly problematic due to contention, interference, and coexistence issues. As a result, current network star-type structuring approaches fail to adequately reconcile IoT application requirements with the underlying devices' fundamental constraints on power, cost, and size [58].

To address the limitations of the start network structure, wireless mesh (multi-hop) networks (WMNs) are widely adopted as an alternative solution [59]. Yet, their current implementations have critical reliability, latency, and security limitations. Considerable research effort has explored how to build and maintain WMNs optimally. To this end, MAC and network layer solutions were proposed, investigating scheduling- and contention-based solutions for the MAC layer and routing protocols at the network layer. Such implementations overcame interference and power-efficiency limitations of start networks at the cost of complex network structures [60].

Selecting between star and mesh structures is scenario dependent, influenced by several elements such as node density, range, environment, as well as power and reliability requirements. In the SUPERIOT project, we aim to adopt a multi-tier network structure, which can have reconfigurable single-hop or multi-hop transmission, harnessing the easy-to-construct advantage of star network and range and power efficiency or mesh networks.

5.2.3 SUPERIOT communication service architecture

A general representation of the network architecture considered in the SUPERIOT project is presented in Figure 2. This multi-tier network architecture may vary from one scenario to another by omitting some of the system components. For instance, in application scenarios where dual EH and dual connectivity are not highly needed, e.g., enhanced label for batch manufacturing, the embedded personal computers (PCs) can be omitted and have a direct connection from gateways/APs to the centralized server. In the following, we detail the protocols used in the different elements of the SUPERIOT network.

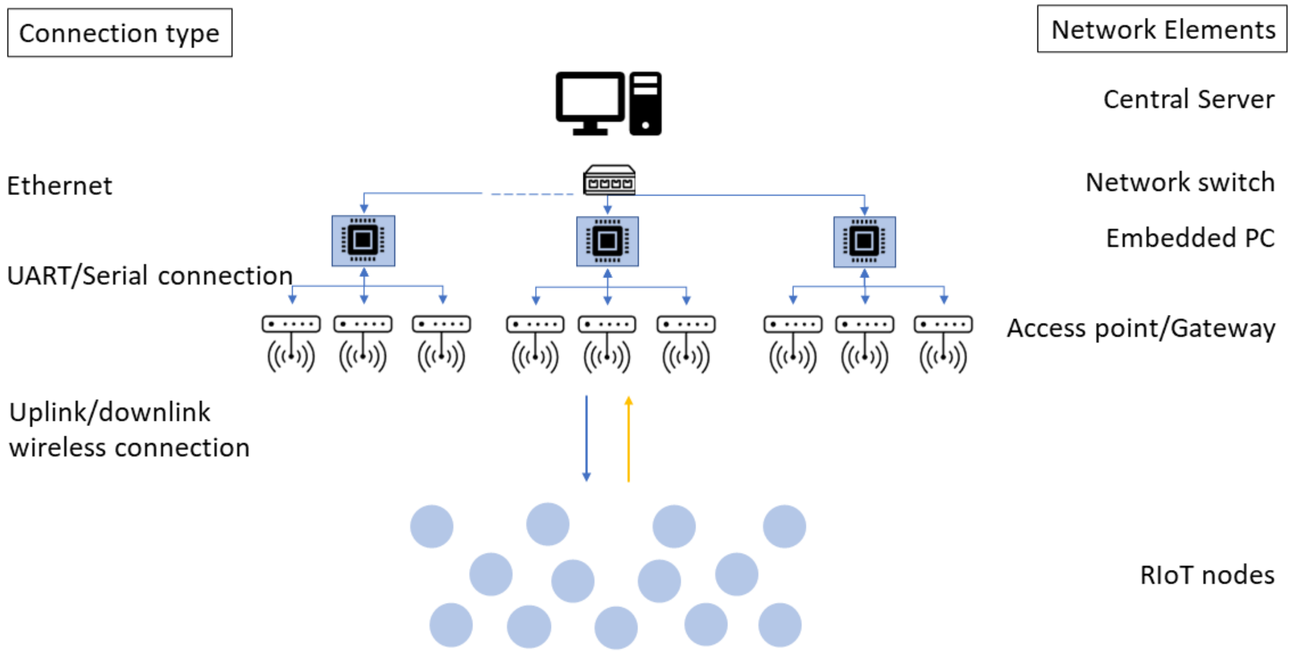

Figure 2: A representation of the general network architecture considered in the SUPERIOT project.

5.2.3.1 Centralized Cloud Server

The centralized cloud server connects all embedded PCs close to the network edge to enable central management, hosting the decision logic for the TX to RX association, logging network elements' behaviour, and maintaining the collected database. Moreover, it can work as an internet gateway to the network, providing connectivity to the embedded PC and RIoT nodes. In SUPERIOT, we will adopt servers running a Linux distribution operating system to allow a smooth development experience due to the wide range of offered language development IDLE platforms and programs in Linux systems. The server connects to the embedded PCs via a secure shell (SSH) protocol [61], a cryptographic network protocol for securely operating network services.

5.2.3.2 Switch/Router

A reliable connection between the Cloud server and the embedded PCs is key to guaranteeing a fast response on data streaming, especially in applications requiring dual high-traffic data flows. The 802.3z Ethernet protocol standard is selected in the SUPERIOT networks based on its capacity to support connections up to 1000 Mbps [62]. The physical Ethernet connection between the server and the embedded PCs is handled using an off-the-shelf network switch, which usually has tens of ports. In application scenarios where an Ethernet connection is not feasible, e.g., due to the long distance from the central server, a virtual router can be initiated on the server offering IEEE 802.11ax Wi-Fi protocol connection with a minimum sufficient transmission rate of 600 Mbps [63].

5.2.3.3 Embedded PC

The embedded PC platform, a.k.a single-board computer, acts as a computation hub between the server and the RIoT nodes. In addition, it can run the MAC layer of the network, processing the channel measurements and forwarding them to the central server. The embedded PC will also be responsible for adapting/controlling the downlink operation of WPT-enabled RIoT nodes, e.g., for SWIPT and SLIPT transmissions.

The embedded PC platform runs an operating system that permits easy implementation of communication algorithms between the server and the gateway segments. Nonetheless, intensive processing tasks cannot be executed on single-board computers, nor can they store big amounts of data. A popular example of embedded PCs is the Raspberry Pi [64], which runs a lightweight Linux-based operating system. Embedded PCs, such as the Raspberry Pi, can compile high-level programming languages such as Python and build, to some extent, ML models. Moreover, they can send/obtain data to/from a Structured Query Language (SQL) database running on the cloud server. The connection from the embedded PC to the gateway/AP can be made via a serial connection, e.g., Universal Asynchronous RX/TX (UART) over Universal Serial Bus (USB). In such a case, a single embedded PC can manage up to 4 AP/gateways, which is the number of USB ports available. Another popular embedded PC is the Beaglebone Black (BBB) microcontroller, which is adopted in applications related to VLC, e.g., the openVLC platform [65]. This BBB board runs a Debian Linux distribution as an operating system.

5.2.3.4 Gateway/Access Point

The gateway, which we also call the AP, is the element in the network that provides connectivity to edge devices, i.e., RIoT nodes. For the case of RF connectivity, we consider Bluetooth Low Energy (BLE), which is one of the main IoT drivers technologies, promising low-energy and low-cost solutions for a great variety of short-range applications, including wearable devices, healthcare, and home automation, to name a few [66]. In a BLE network, the gateway is a master node that manages the connection to multiple nodes (up to seven). BLE system-on-chip (SoC) boards, such as Nordic [67] BLE boards, employ a Real-Time Operating System (RTOS), such as Zephyr RTOS, with its original, fully featured, and optimized stack for BLE-based networks. In addition, Zephyr RTOS has the BLE protocol stack built-in, offering a low-power networking option with adaptable applications over BLE and BLE Mesh. Its more important features are: being highly configurable and modular, supporting cooperative and multiple threading, and having an integrated device driver interface, which allows implementing edge functionalities efficiently, programming the SoC with C and C++ languages.

In the case of the optical gateway, the front-end consists of an LED and a Printed Circuit Board (PCB) to modulate the light level of the LED. They are mounted on a heat sink to regulate the temperature. The front-ends have two operating modes: illumination mode and illumination + communication mode. The control over modulation can be implemented either directly by the embedded PC or by a dedicated micro(controller) on the PCB. More details on the gateway design follow in Section 6.

5.3 Network architecture for localization service(s)

Indoor localization with high positioning accuracy is one of the key functionalities to be provided by the SUPERIOT project. Achieving reliable and high-accuracy indoor localization has been challenging due to the high probability of non-LoS and the rich multipath propagation, resulting in an excessively varying signal strength. Consequently, various localization methods with different advantages and disadvantages are developed based on RF and VLP. The SUPERIOT project aims to improve positioning accuracy by developing a novel localization system based on the joint exploitation of light and radio signals.

In this section, we investigate various localization methods based on light and radio signals and draw the network architecture for localization. To this end, we briefly analyze the requirements first, and then we present the state-of-the-art. Afterwards, we discuss the possible localization service architecture proposed for the SUPERIOT project.

5.3.1 Application requirements analysis

In the SUPERIOT applications document [1], three main scenarios were recognized:

- SUPERIOT-SCN-1: smart tags and labels
- SUPERIOT-SCN-2: large-scale sensing and actuation
- SUPERIOT-SCN-3: enhanced IoT communication in demanding environments.

Providing accurate localization is important for all these three scenarios. Among these scenarios, it is identified that localization is critical, especially for the first scenario, SUPERIOT-SCN-1.

Particularly, from a localization point of view, we define the following high-level requirements for the three main scenarios considered in the SUPERIOT project.

5.3.1.1 SUPERIOT-SCN-1: smart tags and labels

The scenario for smart tags and labels includes applications with smart tags/labels that are used in day-to-day market products, logistic operations, healthcare patient monitoring, medicine and food tracking, and animal monitoring. For this scenario, providing correct localization of the smart tag/labels is critical to help handle procedures in stores and logistics. Similarly, ensuring accurate positioning and localization information of the smart tags is essential to enable monitoring/tracking of the smart tag wearer, such as patients in the hospital or animals on the farm.

5.3.1.2 SUPERIOT-SCN-2: large-scale sensing and actuation

The scenario for large-scale sensing and actuation covers applications such as smart buildings, smart hospitals, smart agriculture and forest, and construction monitoring. Localizing sensors and actuators inside the sustainable IoT nodes helps enable monitoring and track the status of buildings or other structures such as hospitals, bridges, and farms. In addition, dynamically updating the user's location and providing localization information is cooperative for futuristic smart city activities, such as traffic management and transport information.

5.3.1.3 SUPERIOT-SCN-3: enhanced IoT communication in demanding environments

This scenario consists of applications that improve IoT communication in demanding environments with reconfigurable radio-optical IoT nodes and networks. Examples of such demanding environments include underwater, military, and in-body, where secure and private connections are required. Providing accurate positioning and localization of IoT nodes using light and radio signals could bring additional useful information to these environments.

5.3.2 State-of-the-art

Localization is the process of identifying the spatial position of items or people. Providing accurate positioning information is paramount for decision-making in determining the items and individuals. Integrating the Global Positioning System (GPS) and mobile Internet for outdoor localisation has achieved significant success in person and object localization. However, GPS technology has difficulties in indoor applications due to substantial attenuation of the satellite signal and the multipath effect brought on by interference from buildings and the complicated indoor environment [68]. Since the number of IoT devices is expected to increase in future, there is a growing interest in indoor localization techniques [68][69]. Likewise, we recognize that most of the applications highlighted in the SUPERIOT applications document [1] require indoor localization.

In the literature, various techniques have been studied for the indoor positioning system (IPS) by utilizing either radio or light signals. Existing methods based on RF or VLP technology have different advantages and disadvantages [68]-[74]. In particular, RF-based techniques such as BLE, ultra-wideband (UWB), and RF identification (RFID) have a longer operation range and less dependency on the LoS compared to methods based on visible light. Besides, RF technology has the potential to be used under all types of daylight and weather conditions. Thus, RF-based localization methods offer advantages such as versatility, non-LOS tracking, and applicability in both indoor and outdoor settings. However, challenges like signal interference, multipath propagation, accuracy limitations in dense environments, and hardware complexity persist [68]. On the other hand, VLP-based approaches are generally more robust to the multipath interference effect since the optical energy is concentrated on the LOS link [69]. Moreover, VLP-based methods have more available spectrum compared to RF, where efficient frequency sharing to address the challenge of RF spectrum crowding needs to be employed. Furthermore, optical-based localization techniques can be used in RF-sensitive areas since they do not generate radio signal interference. In addition, VLP methods can be employed in areas where wireless communication security is needed since visible light cannot penetrate most objects, and links can be kept confidential [72][73]. Therefore, VLP methods offer several advantages, including high accuracy, low interference, compatibility with existing lighting infrastructure, and utilization in sensitive/confidential areas. However, challenges such as susceptibility to obstacles blocking LoS, limited range, and sensitivity to lighting variations must be addressed.

Within the framework of SUPERIOT, the development of precise localization techniques emerges as a crucial conceptual cornerstone. The fundamental premise herein entails harnessing the advantages of radio and optical communications to facilitate accurate positioning determination. To this end, we review the existing localization methods and categorize them into RF and VLP-based methods as given in the following.

5.3.2.1 RF-Based Localization Methods

RF-based localization methods have gained prominence across diverse applications, ranging from smart tag/label tracking to logistic and animal monitoring. These techniques leverage radio signals to accurately determine the spatial coordinates of objects, devices, or individuals.

RF-based localization techniques rely on the propagation characteristics of RF signals. Key principles include Received Signal Strength (RSS), Time of Arrival (TOA), Time Difference of Arrival (TDOA), Phase Difference of Arrival (PDOA), and Fingerprinting methods. Below we will discuss their working principles and possible drawbacks.

- RSS approaches measure a received signal's power level, enabling distance estimation through signal attenuation analysis. Existing methods based on RSS can be found, among other sources, from [75]-[77]. These approaches often use trilateration techniques with at least three known base stations to offer positioning in a two-dimension space. However, RSS methods require proper propagation channel modelling for accurate estimation, and hence they significantly suffer from the multipath and shadowing effect. Moreover, the gain and radiation patterns of the antennas are unknown in most scenarios. In addition, any orientation or rotation of the tag/label causes radar cross-section (RCS) variation in time, and thus RSS methods alone are not reliable in many practical applications [78].
- Another technique for localization is employing the time of flight (TOF) concept. Such techniques use the propagation time of the RF signal, and TOA and TDOA are two common methods for the TOF principle [78]-[80]. TOA approaches calculate the distance between a TX and an RX based on the time the signal travels between them. In this concept, the electromagnetic wave speed may be multiplied to get the distance between the reader/base station and the IoT node. Then the node can be positioned using trilateration or other techniques. In TDOA approaches, the time difference between the arrival of a signal at multiple RXs is measured to enable trilateration for accurate position estimation. However, methods based on TOA and TDOA require accurate time measurements, i.e., high synchronization between TXs and RXs, which can be difficult to implement in low-cost and low-power networks. Moreover, these methods demand high signal bandwidth to secure acceptable positioning precision in multipath environments [68].
- The phase information of the received RF signal can also be used to measure the distance/angle. Such localization methods rely on the PDOA between multiple signals. They are usually categorized under three principles, i.e., time domain phase difference of arrival (TD-PDOA), frequency domain phase difference of arrival (FD-PDOA), and spatial domain phase difference of arrival (SP-PDOA) [71][81]-[83]. TD-PDOA measures the phase of two received signals at two different time instances and estimates the projection of the node velocity vector onto the line of sight between the node and the reader. Thus, it may be considered a method of detecting Doppler shift to find the node's speed. However, the TD-PDOA approach requires the movement of the tag/node, which might not be available for many applications. In FD-PDOA, the reader/network will measure the phase of the received signals at different known frequencies, and based on the phase difference between these frequencies, the distance can be calculated by the derivative of the phase difference for the frequency difference. Thus, such a method may be considered a frequency-modulated continuous wave radar and can work for both

moving and stationary targets. FD-PDOA approach shows promising potential for accurate localization; however, they require high instantaneous bandwidth to overcome the ambiguity and extend the detectable range. In the SD-PDOA approach, angle of arrival (AOA) information can be estimated using the reflected signal's phase differences at several receiving antennas. Thus, it can be considered a direction of arrival estimation using a phased array antenna. SD-PDOA approaches demonstrate promising results, and many signal-processing techniques have already been established to improve angle estimation accuracy [83]-[86]. However, they are sensitive to the multipath fading effect. Moreover, they increase the physical size of the reader/network as they require multiple receiving antennas.

- In addition, there are also methods based on fingerprinting and likelihood statistics [87][88]. Fingerprinting methods create a dataset with pre-measurements and then match or predict the nodes or target’s coordinates according to this dataset. Such fingerprinting methods and statistical models can also be used to train ML to improve estimation accuracy. Fingerprinting methods are often performed in two steps, i.e., the offline phase and the online phase. The dataset can be built to train an ML model in the offline phase. The node's location can be estimated by comparing the measured metrics with the records of the reference information in the database during the online phase. However, fingerprinting methods require an appropriate and huge dataset for acceptable accuracy.

Recent advancements include the integration of ML algorithms for enhanced accuracy, fusion of RF with other sensor data for improved performance, and the development of advanced antenna arrays for better signal processing. These advancements will likely improve localization accuracy, reduce latency, and enhance real-time capabilities. RF-based localization methods have revolutionized various industries by enabling precise spatial positioning and tracking. As technology advances, RF-based solutions such as BLE and RFID will play an increasingly integral role in shaping the future of navigation, communication, and the IoT. Addressing existing challenges and harnessing forthcoming opportunities will undoubtedly contribute to refining and enhancing RF-based localization methods.

5.3.2.2 VLP-Based Localization Methods

VLP-based localization techniques have emerged as a promising technology for accurate positioning and tracking applications. These approaches utilize the modulation of visible light signals to determine the precise location of objects and individuals. Similar to RF technology, key principles of VLP-based localization can be categorized as RSS, TOA, TDOA, AOA, and Fingerprinting. Below we will discuss their working principles and possible drawbacks.

- RSS is the most straightforward VLP method, as the received light intensity information is usually available using a single photodetector and without requiring complex hardware [89]. These methods measure the incident optical power for each observed optical beacon and perform trilateration to estimate the target’s location. The challenge herein is that the optical propagation channel must be modelled appropriately to obtain sufficient accuracy with RSS-based VLP methods. RSS-based methods suffer from increased position error when the received optical signal has variations in the power levels and radiation pattern due to physical environmental changes [69].
- TOF methods, such as TOA and TDOA, deal with the drawbacks of RSS-based positioning by using the relationship between the distance and signal propagation delay. Such methods measure the time light signals require to travel between the TX and RX and then apply trilateration to find the position. TOF approaches can provide low position errors but are sensitive to time offset and demand precise synchronization between TXs [72].
- Another VLP approach is to use fingerprinting-based localization [73]. These approaches compare the received signal with the existing record in the dataset. However, they are susceptible to environmental changes and require stable received signals and large data sets.

- AOA-based VLP approaches exploit spatial diversity between multiple RXs to determine the relative angle between the RX and the node. After measuring the angle at which light signals arrive at multiple sensors, they perform triangulation to estimate the position between the optical beacons and RX. Generally, AOA techniques are more robust against TX nonidealities and transmit power variations [72]-[74]. Moreover, AOA-based VLP systems do not require precise signal strength measurements and time synchronization between TX and RX. Therefore, they can overcome the drawbacks of RSS and TOF-based approaches. However, the main challenge for the AOA-based approach is that they usually require more complex RXs, such as cameras, compared to photodiodes, and they might not be suitable for fully printed IoT systems.

Recent developments in VLP-based localization methods include improved algorithms for increased accuracy, IoT platform integration, and multi-modal approaches combining visible light with other technologies like RF. VLP-based localization methods present a promising avenue for accurate and reliable positioning, particularly in indoor settings [69]. Addressing signal obstructions and hardware requirements challenges will be crucial for broader adoption as technology evolves. With applications spanning from indoor navigation and retail analytics to healthcare and transportation, VLP-based localization has the potential to reshape various industries by providing precise and context-aware positioning capabilities.

5.3.3 SUPERIOT localization service architecture

In the previous sections, we discussed the requirements of the potential applications and reviewed the state-of-the-art for localization methods. To the best of our knowledge, we believe the localization system will agree with the general representation of the network architecture presented in Figure 2. We divide existing localization methods into two categories: RF-based and VLP-based.

RF-based localization methods play a vital role in diverse applications, enabling accurate spatial determination using RF signals. While standalone RF methods offer numerous advantages, addressing challenges such as signal interference and accuracy in complex environments remains a focus of ongoing research. As technology evolves, RF-based localization methods are expected to continue enhancing various industries, ranging from indoor positioning and IoT management to animal and transportation monitoring. Various RF technologies exist, such as Wi-Fi, UWB, BLE, and RFID. Among them, we find BLE and RFID tags to be the most suitable options for semi-printed and fully printed IoT due to low power constraints. For these RF technologies, we consider SD-PDOA and FD-PDOA as the most promising techniques for RF-based localization services to ensure high positioning accuracy.

VLP-based localization is also a promising alternative indoor localization method, as it provides high positioning accuracy and low interference. Moreover, it allows for utilizing the existing lighting infrastructure, and the rapid increase in the usage of LEDs provides the advantage of lower cost. Therefore, with ongoing research and innovation, VLP-based localization is poised to play a pivotal role in shaping the future of precise positioning and tracking systems. However, no dominant VLP-based localization system has yet been identified for the SUPERIOT project. The AOA-based approach demonstrates very good results and is considered one of the most promising candidates for the VLP systems. The main advantage of an AOA-based VLP system is that the accuracy relies on identifying a given light source instead of the signal strength or frequency of the modulated signal. However, such an approach, by default, requires camera-based RX. For the semi-printed and fully printed IoT nodes, a photodiode-based RX is planned to be used. Therefore, as a standalone VLP system, an RSS-based approach with a single photodiode could be more suitable for the SUPERIOT project.

Dual-mode sensor fusion with RF and visible light will combine the advantages of both standalone systems and enhance the accuracy of the positioning system. During the initial studies for the SUPERIOT project, joint utilization of received AOA and RSS measurements from both RF and light sources is considered to develop a highly reliable and energy-aware localization system for mobile IoT nodes. Moreover, the design of an appropriate Bayesian filter with adaptive weights could be investigated to combine AOA and RSS measurements optimally at the nodes.

5.4 Network architecture for energy transfer service(s)

The concept of "true sustainability" promoted by the SUPERIOT project introduces substantial implications for the energy autonomy of the nodes. Not always minimization of energy consumption is sufficient to ensure efficient long-term operation. One possibility to address this challenge is enabling a node to recover its energy by scavenging it from ambient sources or purposeful energy transmissions (i.e., energy transfer[7]).

In the rest of the section, we discuss and sketch the network architecture of the energy transfer service for SUPERIOT. We start by analyzing the requirements, then briefly discuss the state-of-the-art and present and discuss the energy transfer service architecture proposed for the SUPERIOT project.

5.4.1 Application requirements analysis

The SUPERIOT applications document [1] identified three major classes of applications, namely (i) SUPERIOT-SCN-1: smart tags and labels, (ii) SUPERIOT-SCN-2: large-scale sensing and actuation, and (iii) SUPERIOT-SCN-3: enhanced IoT communication in demanding environments. Though energy autonomy has been identified as an important requirement for the applications in all three classes, it was essential for the first class - SUPERIOT-SCN-1. Therefore, Table 3 summarises the energy scavenging and storage requirements for the respective applications. Meanwhile, for SUPERIOT-SCN-2 and SUPERIOT-SCN-3 though energy scavenging is also expected to be extensively used [1], some energy buffer (e.g., a battery) is envisaged to be available on the nodes to increase operation reliability and tackle the possible periods of scavenged energy unavailability.

Notably, it can be seen that the energy scavenging from RF signals is expected to be used more extensively by the potential applications than the energy scavenging from optical. One of the reasons beyond this is that some applications imply positioning devices in areas where ambient or purposely-generated light is impossible (e.g., inside the building walls – application 2.2).

Table 3. EH and storage requirements for SUPERIOT SUPERIOT-SCN-1 applications identified in [1].

Application ID(s) in [1][8]	Scavenging		Energy storage in a battery
	RF	optical	
1.1,1.2	v	v	-
1.3-1.5,1.7,1.11	v	-	-
1.6,1.9	v	-	v
1.10	-	v	v
1.7	-	-	v

Importantly, neither of the applications listed in [1] explicitly implies purposeful energy transfers over RF or VLC – the energy for operation can be harvested from ambient sources (e.g., third-party systems such as WiFi routers or conventual lights, which are widely available in office-like environments) available in the operation environment. As discussed above in Section 5.1, many of the applications are expected to be deployed in environments where other systems, signals of which can be used as "energy donors", will be operating. The advantage of this approach is

[7] In this document, we use the term "energy transfer" to denote the purposeful transmission of a signal (e.g., RF or optical) for energy being collected or scavenged from it.
[8] For the sake of convenience and self-sufficiency, the list of scenarios and applications identified in [1] is provided in Appendix 1.

that it effectively simplifies the overall design of the network and removes the need for supporting any energy transfer. However, the main downside is that it makes energy scavenging more random, unpredictable and opportunistic. Considering this, some limited experiments and developments focused on energy transfer are foreseen within SUPERIOT, as discussed below.

5.4.2 State-of-the-art

The general-level information about EH and energy transfer from ambient sources, RF and light, among other sources, can be found from [90]-[96]. Below we will discuss them and the recent trends.

In recent decades, energy scavenging from natural (e.g., the Sun) and ambient (e.g., lamps) has been widely used to power low-power electronics. One of the primary reasons for it is the relatively high compared to other sources of ambient light energy density. To give a numeric example, while ambient RF signals have an energy density below 1 $\mu W/cm^2$, the density of the ambient light reaches 100 $\mu W/cm^2$ and 100 mW/cm^2 under office illumination and direct sunlight, respectively [90][96]. Another reason is that photovoltaic (PV) technology, which allows to transform the light into DC, is already well established and demonstrates relatively high efficiency [97] compared to harvesting energy from other sources.

The recent trends related to the materials for PV energy scavenging are extensively discussed in [96]. However, surprisingly, energy transfer using light, especially in the Internet of Things (IoT) context, has not been extensively explored. One of the few works suggesting using a controllable visible light source for charging IoT devices is reported in [98]. The authors conceptualized and implemented a link between the IoT devices and the intelligent lamps in the office environment, allowing the former to request light turns on. The laser-based energy transfer has been widely explored and conceptualized in space and space-to-ground communication, as discussed in [99]. Notably, the PowerLight (and its predecessor LaserMotive) company even offers a commercial solution implementing laser-based energy transfer [100] and has demonstrated a beam-power propulsion mechanism to power an unmanned aerial vehicle [101]. However, to the best of our knowledge, no specific standards regulating light-based energy transfer exist today.

RF-based energy transmission is much more widely used for energy transfer to IoT devices. An up-to-date overview of the respective technologies and challenges is provided in [102], including references to some practical implementations. Among the fundamental difficulties for practical utilization of RF-based wireless energy transfer can be listed:

- The limited transmit power due to the frequency regulations and the need to avoid any possible negative impact on living beings and interference with external systems.
- High attenuation with distance obstructing omnidirectional energy transfer and typically low energy efficiency of non-directive RF-based energy transfers. Notably, the RF signal power and waveform often affect the efficiency of the RF to DC conversion.

Unlike other types of wireless energy transfer (i.e., inductive or conductive), to the best of our knowledge [102], the standardization of the RF-based energy transfer has just recently commenced in the AirFuel Alliance (AirFuel RF), NFC Forum (Wireless Charging Specification 2.0) and the Association of Radio Industries and Businesses (ARIB STD-T113) in Japan. Still, no ready standards exist at the current time. Commercial products for wireless power transfer are offered, e.g., by the Powercast company [103]. It should also be noted that most of the existing RF-based wireless prototypes and solutions imply omnidirectional energy transmission or point-to-point transmission. Implementation of the point to multipoint transmissions, though they have been conceptualized and studied analytically, is not known to us.

The node-level hybrid energy scavenging solutions capable of harvesting energy from multiple sources, including RF and VLC, have already been presented (e.g., in [104]). The optimization of such networks has also been approached in some studies (e.g., in [105]-[107]), though mostly often the authors implied that only one modality (mostly often – light, due to the reasons discussed above) is used for providing power to the devices. To the best of our knowledge, none of the experimental testbeds demonstrating networked hybrid VLC and RF-based wireless energy transfer has been demonstrated yet.

5.4.3 SUPERIOT energy transfer service architecture

In the previous sections, we discussed the requirements of the potential applications and the state-of-the-art for wireless energy transfer. Based on these, the following approach was selected for the SUPERIOT energy transfer architecture.

RF-harvesting RIoT sensors will have three communication protocol phases: EH, Downlink (DL) communication, and uplink Backscattering. In the case of RF energy transfer, the gateway will adapt the downlink signal depending on the desired wireless power transfer mode at the RIoT node. The SUPERIOT project adopts multi-tone signals for wireless power transfer (cf. Deliverable 2.1). In the case of the SWIPT RIoT node, the gateway downlink signal will be transmitted with multi-tone modulation, which is the case for Gaussian frequency-shift keying (GFSK) used in BLE. In the case of wireless power transfer via backscattering, the gateway will simply propagate a multi-tone signal for the RIoT node to backscatter. Switching between the two modes will be done in the baseband of the embedded PC. Software-defined radios (SDRs) will also be considered to resemble coexisting TXs in the environment, which can introduce extra ambient RF signals that can be harvested. It is worth noting that such SDRs are not part of the SUPERIOT network but are rather part of the environment.

In the case of optical communication, energy transfer can be done by exploiting the illumination of the APs' LEDs, and using RIoT nodes equipped with PV cells. SUPERIOT investigates two approaches for light-based EH. In the first approach, we consider LEDs at the AP side set in joint illumination and communication OOK mode. In this mode, the total light intensity should be comparable to the illumination mode only, so the user does not observe any illumination difference, enabling SLIPT. No extra software requirements are needed at the gateway for this mode, and the energy transfer efficiency mainly depends on the quality of the PV cells at the RIoT. In the second approach, we aim to further improve the EH efficiency by introducing a pulse-shaping waveform for the SLIPT scenario in the SUPERIOT gateway design. From the node side, only a PV cell is required, where the bandwidth of a PV-equipped IoT device will be the only limitation factor in this case. The pulse shaping scheme can be implemented in the baseband and controlled on the gateway's embedded PC (cf. Chapter 8).

5.5 Integrated network architecture

In Sections 5.2-5.4, the architectures of three services or functionalities, namely communication, localization and energy transfer, which compose the overall SUPERIOT network architecture, have been discussed separately. However, this is obvious that the elements of the network architecture implementing different functionalities can be integrated, thus reducing the overall number of the devices composing the network, paving the way to reducing material and energy consumption, and thus increasing sustainability. Notably, the three discussed services are interdependent, and next, we show just several most illustrative connections between them:

- *Communication and localization services.* Whatever principle of wireless localization is used, the exchange of some data (at a minimum – making the RX aware of the unique identifier of the TX which has sent the signal, its geoposition, and some relevant information about the signal, such as the transmit power or timestamp) is often implied and required to enable localization or increase its accuracy. Wise versa, the information about the location and mutual positions of the devices provides important insights for optimizing the communication between these devices, especially for selecting the optimal communication modality (RF or optical signal) and parameters (e.g., the bandwidth, transmit power, modulation-coding scheme). Notably, in some cases, the conventional communication frames can be used to enable localization either as they are or with some modifications, which boosts the efficiency of time-frequency resource utilization.
- *Communication and energy transfer services.* Likewise, the localization, the communication can benefit to implementation of energy transfer, e.g., by enabling an energy RX to provide feedback to the TX on the amount of energy it receives. The

communication, in turn, can consider the available energy and energy income prognosis for routing, scheduling the resources, and optimizing the communication parameters.

- *Localization and energy transfer.* Obtaining accurate positioning information might be even more important for energy transfer than for communication to assess the feasibility and efficiency of wireless energy transfer. The value of accurate localization increases even more if directive energy transmission is to be employed.

Therefore, integrating the different functionalities should be carefully considered, accounting for both the pros and cons. Overall, the integration of the different functionalities and support of them by network elements is expected in the SUPERIOT network at the latter stages of the project. For this reason, implementing the functionalities should be based on the same principles, hardware and software components, and interfaces and follow the modular approach whenever possible. However, to speed up and parallelize the work during the early phases of the project, the development, implementation and experimental validation of the different functionalities are expected to be carried out in parallel. Notably, to facilitate the integration, the interfaces between the functionalities will be focused on and specified at the next phase of project execution.

Importantly, as discussed in Sections 5.3 and 5.4, the network architecture designs envisaged for localization and energy transfer service do not contradict each other, and the design of the communication architecture is presented in Section 5.2 and depicted in Figure 2. Even more, the previous discussion shows the high similarity between the different functional architectures, thus enabling their seamless integration.

5.6 Analysis of the energy budget and discharge rate

The node budget refers to the total energy consumption of the IoT device, accounting for all active components such as BLE and VLC transceivers, sensors, and the E-ink display during a complete operational cycle. Each component's energy requirement is determined by its power consumption and the time it remains active. The discharge time of the supercapacitor powering the node is influenced by the average power demand of the node and the supercapacitor's capacity. It can be estimated using the relationship between the supercapacitor's capacitance, the initial and minimum operating voltages, and the node's average power consumption. This discharge time defines how long the device can operate before requiring recharging or EH input. Understanding the node budget and discharge times is crucial for ensuring sustainable operation and optimizing the design of energy storage and harvesting systems. We analyze the energy budget of the Si-based reference node considering any current optimizations that have been performed to date. For more details about the methodology of the analysis please refer to SUPERIOT deliverable D2.1.

Let's consider the following two scenarios, representing illustrative extreme cases:

1) **Scenario 1**: Node is connected via BLE to a central device throughout its whole operation and performs sensing, E-ink displaying, and VLC TX/RX (including idle period) in one cycle every **1 hour** or **1 min**. The node does not sleep at any point in time during its operation (see node operations in Table 4).

2) **Scenario 2**: Node operations include startup, sensing and E-ink displaying, and deep sleep in one cycle, which is repeated every **1 hour** or **1 min** (see node operations in Table 5).

Table 4. Node's operation cycle with all functionalities enabled.

Operations	**Current (mA)**	**Duration (s)**	**Energy (J/cycle) @ 3.3 V**
Sensing	8.76	0.516	0.0149
E-ink display	4.12	0.435	0.00591
VLC TX/RX	8.15	0.1	0.00269
Idle	2.245	3598.949/58.949	26.66 / 0.437
TOTAL (1 hour cycle/1 min cycle)			**26.69 / 0.46**

Table 5. Node's operation cycle with both BLE and VLC turned off.

Operations	**Current (mA)**	**Duration (s)**	**Energy (J/cycle) @ 3.3 V**
Startup	15.1	0.910	0.0453
Sensing	13.4	0.149	0.00659
E-ink display	3.2	0.544	0.00574
Deep sleep	0.005	3598.397/58.397	0.0594 / 0.000964
TOTAL (1 hour cycle/1 min cycle)			**0.117 / 0.0586**

Only part of the supercapacitor's stored energy is available to applications because, at some stage of discharge, the voltage becomes too low to be useful. The effective energy stored in the supercapacitor is given by:

$$E_{\mu C} = \frac{1}{2} C (V_{\text{initial}}^2 - V_{\text{shut}}^2)$$

where

$E_{\mu C}$ is the energy stored in the supercapacitor in Joules,

C is the capacitance of the supercapacitor in Farads,

V_{initial} is the initial voltage or charged capacitor's voltage (3.3 V),

V_{shut} is the shutdown voltage or minimum voltage at which node is still operational (1.6 V).

Therefore, considering the targeted supercapacitor capacitance of 14.7 mF, the effective energy stored in the supercapacitor is given by:

$E_{\mu C} = \frac{1}{2} \times 0.0147 \times (3.3^2 - 1.6^2) = 0.0612$ J.

The voltage drop on the supercapacitor during the current flow is given by:

$V_{\text{drop}} = I \times ESR$ or $V_{\text{drop}} = I \left(ESR + \frac{t}{C} \right)$

where

I is the current (A).

ESR is the equivalent series resistance (ohms),

t is the time (seconds)

C is the capacitance of the supercapacitor (F).

We consider the constant current discharge, where constant current implies that the application consumes a stable current as the voltage falls during the discharge. Applied resistance should vary to achieve a constant current regardless of the applied voltage.

Discharge time, $t = \frac{C(V_{\text{initial}} - V_{\text{shut}})}{I}$.

The initial voltage of the supercapacitor is set as V_{initial}=3.3 V. Considering the targeted supercapacitor capacitance of 14.7 mF, the discharge time for each scenario (see Scenario 2: Node operations include startup, sensing and E-ink displaying, and deep sleep in one cycle, which is repeated every **1 hour** or **1 min** (see node operations in Table 5).

Table 4 and Table 5) are given in Table 6.

Table 6. Discharge time of 14.7 mF supercapacitor for each scenario.

Scenario (cycle duration)	Average current consumption (mA)	Discharge time (s)
Scenario 1 (1 hour)	2.25	11
Scenario 1 (1 min)	2.32	10
Scenario 2 (1 hour)	0.01	2536
Scenario 2 (1 min)	0.3	84

It is evident from Table 6 that the targeted supercapacitor size of 14.7 mF will quickly drain its energy, especially for scenario 1 where the energy consumption is higher. For both scenarios, regardless of the high-frequency or low-frequency activity patterns, the 14.7 mF supercapacitor will not have enough energy to complete one operational cycle. For scenario 2, the discharge time is much longer since the node enters deep sleep (with very low energy consumption) after completing its active operations at the start of the cycle. Thus, to ensure continuous node operation, enough energy needs to be harvested to charge the supercapacitor during the node's idle or deep sleep periods, so that the node will have enough energy to complete the active operations (e.g. sensing, E-ink displaying, VLC TX/RX) at the start of each duty cycle. Therefore, it is critical to evaluate the feasibility of EH from three potential sources: (i) ambient light, (ii) visible light communication (VLC) and (iii) RF via wireless power transfer (WPT).

(i) **Energy harvesting from ambient light**: In-line with the assumptions of D2.1, we consider the current version of an organic photovoltaic (OPV) solar cell with an effective power density of 27 μW/cm² under 1000 lux illumination. We expect the supercapacitor to charge during the idle or deep sleep periods. We need to calculate the solar panel area required to generate enough energy during the idle or deep sleep periods to fully charge the supercapacitor. Thus, we need to consider the energy consumed during the idle or deep sleep periods, in addition to the extra energy needed to charge the supercapacitor to its maximum capacity. The OPV cell size needed to provide the required output power to charge the supercapacitor fully is given by

$$\text{OPV solar cell size} = \frac{E_{\text{total}}}{\text{OPV power density} \times \text{charge time}}$$

where E_{total} is the total energy consumed by the node in each operation cycle.

Using the energy values in Table 4 and Table 5, we compute the minimum required solar cell sizes in Table 7 that will provide enough power to charge the supercapacitor to ensure continuous node operation.

Table 7. Computation of minimum OPV solar cell size for each scenario.

Scenario (cycle duration)	Average power required (uW)	Min. solar cell size required (cm²)
Scenario 1 (1 hour / 1 min)	7412 / 7671	275 / 290
Scenario 2 (1 hour / 1 min)	33 / 978	1.3 / 38

(ii) **WPT over VLC**: The illumination mode of the optical communication gateway's front end will be employed for light-based energy transfer. Measurements conducted using a white LED, with both DC (illumination) and communication (PWM) power consumption maintained at 2 W, produced intensities of 800 lx and 750 lx, respectively. As per Section 8.3 and Figure 14, the maximum measured harvested power is around 145 uW using only DC, and around 135 uW with DC and PWM.

Let's consider the maximum power harvested, $P_{\mathrm{harvested}}$=145 uW. The total energy harvested, $E_{\mathrm{harvested}}$ over 1 hour and 1 min periods would be equal to 0.522 J and 8.7 mJ, respectively. Referring to scenario 1, the energy harvested is far less than the energy required to sustain the node's operations in each cycle. As for scenario 2 where BLE and VLC are disabled (see Table 5), the harvested power of 145 uW will be able to charge the supercapacitor during the deep sleep period. However, for the high frequency activity pattern (1-min cycle), the supercapacitor will not have enough time to charge to its maximum capacity as illustrated in Figure 3(a), and the node will be able to perform only part of the active operations at the start of the second cycle before shutting down. As for the low-frequency activity patterns, that is, 1-hour cycle in scenario 2, the harvested energy will be enough to sustain continuous node operation, as shown in Figure 3(b).

Note, that the power consumption of the AP for providing this power is around $P_{\mathrm{AP\ consumed\ VLC}}$=2W. However, this is worth noting that this power consumption should be considered with care, as it combines the power for WPT, communication and generating light (e.g., for human users use). Therefore, if implemented as a part of the conventional light fixtures and operated when light is on, this will not inquire additional energy consumption.

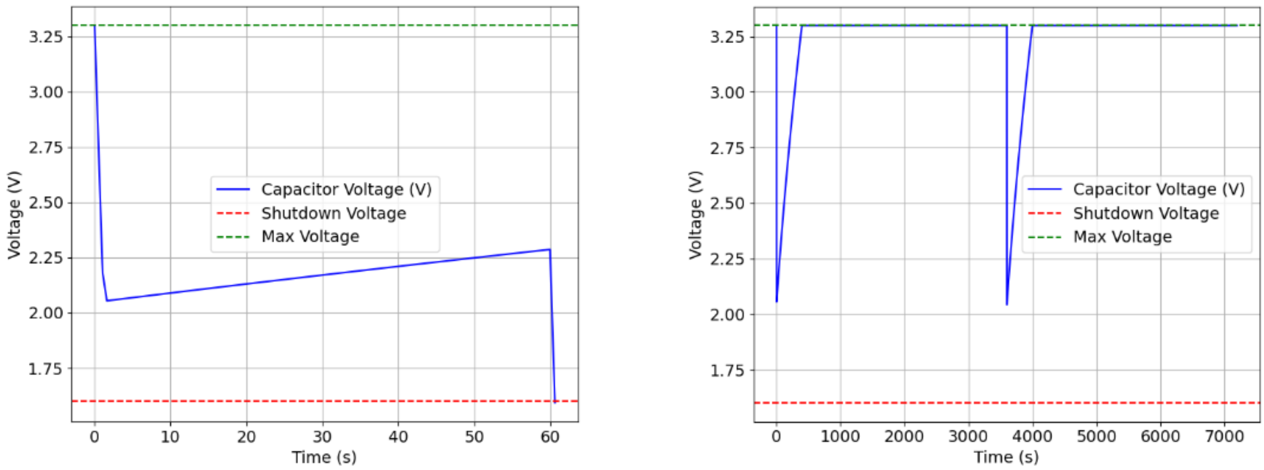

(a) (b)

Figure 3: Supercapacitor discharge profiles for scenario 2, considering harvested energy from WPT via VLC: (a) 1-min cycle, (b) 1-hour cycle.

(iii) **WPT over RF:** RF EH was evaluated as a potential energy source to sustain the continuous operation of the IoT node. Using a 2.4 GHz RF TX with a maximum transmission power of 30 dBm and a dipole antenna with a gain of 2.15 dB, the harvested power at 1-meter distance is calculated as follows:

Transmit power, P_{TX}=30 dBm = 1 W (AP's power consumption=1 W/0.7=1.43 W considering a 70% DC to RF conversion efficiency).

The Free Space Path Loss (FSPL) is calculated as follows:

$$\text{FSPL} = 20\,log_{10}(d) + 20\,log_{10}(f) + 20\,log_{10}\left(\frac{4\pi}{c}\right) - G_t - G_r$$

where

d is the distance in metres (m),

f is the frequency in Hz,

c is the speed of light in m/s,

G_t is the TX gain in dB, and

G_r is the RX gain in dB.

Thus, if d=1 m, f=2.4 GHz, c=3x10^8 m/s, G_t=G_r=2.15 dB, the FSPL=35.74 dB.

The received power is thus given by:

$$P_{\text{RX}} = P_{\text{TX}} - FSPL = 30\,dBm - 35.74\,dB = -5.74\,dBm = 0.267\,mW$$

The RF to DC conversion efficiency is ~30% at -6 dBm [108]. Therefore, the harvested power is given by:

$P_{\text{harvested}}$=0.3 x P_{RX}= 0.3 x 267 uW = 80.1 uW.

Considering a supercapacitor charging efficiency of 95%, the effective harvested power, $P_{\text{harvested}}$=76 uW. Comparing this value with the average power required for continuous node operation in Table 7, we observe that the amount of power harvested from the RF source can only ensure continuous node operation for Scenario 2 with the low-frequency activity pattern (i.e. 1 hour duty cycle). However, we anticipate that the performance of RF EH can be significantly enhanced using directive antennas and multi-stage rectifier circuits. Directive antennas focus the reception of RF energy in a specific direction, increasing the power density and reducing path loss, which is particularly beneficial when the RF source is stationary, or its location is known. Multi-stage rectifier circuits further improve efficiency by effectively converting weak RF signals into usable electrical energy. By cascading multiple rectification stages, these circuits maximize the RF-to-DC conversion process, enabling better utilization of both ambient and dedicated RF signals. Nonetheless, the RF regulations, which were designed having wireless communication and not WPT in mind, can introduce limitations for the maximum transmit power, duty cycle or the possibility of using directive antennas.

When this comes to AP's energy consumption, to generate 1 W (30 dBm) radio power the signal generated by the radio transceiver has to be usually amplified by a dedicated power amplifier, the power consumption will prevail in the total energy consumption. Considering the characteristics of realistic power amplifiers (e.g., SST12CP33), the typical power consumption for generating 30 dBm will be $P_{\text{AP consumed RF}}$= 440 mA x 5 V = 2.2 W.

In our approach, we are leveraging three complementary EH technologies: WPT over VLC and RF, and ambient light harvesting. WPT over VLC enables simultaneous data transmission and energy transfer using visible light, which is highly efficient in LoS scenarios. WPT over RF, on the other hand, supports EH over longer distances and in non-LoS environments. Ambient light harvesting through OPV complements these methods by converting natural or artificial light into electrical energy, making the system versatile and adaptable to different operational environments. By combining these techniques, the hybrid EH system will ensure robust and resilient energy generation for the RIoT nodes.

5.7 Reconfigurability and reusability aspects

Reconfigurability and reusability are critical to ensure that the SUPERIOT solution remains valuable and efficient in long-term operation. Besides, flexibility and uniform design are crucial to facilitate the integration of the different functionalities together, as was discussed in the previous section. To support this, the following aspects will be considered:

- *Well-established hardware/software ecosystems*, which availability and support will likely continue in the future. This affects the selection of the hardware and software components to be used, including the integrated development environment (IDE) and programming languages which will be used for implementing SUPERIOT devices and their firmware/software.
- *The modular design of hardware/software* allows updates and upgrades of the individual hardware and software components to keep the functionality of the SUPERIOT devices and network up-to-date with the state-of-the-art. Besides, modular design can substantially simplify the further integration of individual components and functionalities. This requires accurate specification of the interfaces between the different modules and documentation of the designs.
- *Open publication of the developed designs and codes and proper documentation* would also be carefully considered to create a community around the SUPERIOT platform, allowing other stakeholders to benefit from our developments while increasing the platform's capabilities through development done by third parties for their needs.
- *Accurate specification of the network architecture and interfaces between the network infrastructure elements* is crucial to ensure the overall scalability and compatibility of the elements developed in various tasks by various parties.

These aspects will be considered when developing the overall SUPERIOT network architecture and its elements (e.g., the gateway, as discussed in the next section). Notably, this flexibility is important to ensure the overall sustainability goal targeted by the SUPERIOT project, regardless of how the sustainability metrics of individual application or use case might look like.

6 Network simulations

This section presents the design and implementation of network-level simulations conducted to evaluate the proposed architectures. The primary objective of these simulations is to analyse the performance of different network configurations, addressing critical factors such as throughput, communication reliability, and scalability. The study incorporates simulations using state-of-the-art models in ns-3 to assess key performance metrics under realistic conditions.

We start this section by reviewing the state of the art in ns-3 models, focusing on BLE, OWC, and energy modelling capabilities. Then, we examine the preliminary performance of BLE, analysing link behaviour under varying conditions such as distance, transmission power, and network size. Next, we explore energy modelling, investigating EH, storage, and consumption mechanisms using Wi-Fi as a reference. Finally, we summarize the main findings, highlight limitations in the current models, and discuss next steps for refining the models.

6.1 State of the art analysis on ns-3 models

6.1.1 Bluetooth Low Energy

BLE integration within the ns-3 platform remains an emerging area, with official support yet to be established. Currently, the primary publicly available BLE module is a master's thesis project from 2018 by Stijn Geysen at KU Leuven University [109]. This module, available through the author's GitLab repository, comes with a disclaimer regarding potential errors and a lack of ongoing maintenance. The challenge is further compounded by sparse documentation, making thorough evaluation difficult. Initial experiments with this module exposed various errors and instabilities, necessitating porting to the latest version of ns-3. Substantial adjustments were required to render it minimally functional.

This module’s architecture follows a design inspired by the community-driven LoRaWAN module, which is a well-established framework widely used for various IoT applications. While LoRaWAN and BLE are quite different in terms of protocol and application, the module leverages this architecture as a foundation for its implementation.

Building on this, we observed that the module was primarily designed for research into Bluetooth Mesh networking. However, the author did not aim to strictly adhere to the Bluetooth standard. Instead, the implementation, based on BLE version 4.2, simplifies several aspects of the protocol. For example, many features of the Generic Attribute Profile and application layers are not implemented, making it impossible to establish standard connections or perform device discovery. Additionally, compatibility with other ns-3 applications is severely limited. The module’s broadcast-oriented approach requires significant adjustments to integrate with existing ns-3 tools, limiting our ability to extract connection metrics from simulations.

On the PHY layer, the module deviates from the standard GFSK modulation, opting instead to implement the Offset Quadrature Phase Shift Keying (OQPSK) which differs significantly from the standard. Additionally, the PHY layer only supports 1 Mbit/s of bit rate, necessitating the implementation of 2M. At the MAC layer, simplifications include a restricted connection interval, where only one packet can be sent per transmission window, in contrast to the standard, which supports multiple packets per interval.

Despite the module’s limitations, there are some functional aspects worth highlighting. The provided BLE applications enable traffic generation, simulating scenarios where a sensor collects and broadcasts data. However, the implementation is limited to a mesh network where every node connects to every other node, with no control over the network topology. This fully connected structure works out of the box but lacks the flexibility to customize or optimize the network. All data transmission occurs via broadcast, as no connection-oriented protocols are implemented. While this allows for basic communication in a mesh setup, it also limits the scope of potential use cases. Furthermore, due to the module’s lack of compatibility with standard ns-3 tools, extracting meaningful metrics from these connections is very challenging. For example, tools like FlowMonitor are incompatible, making performance evaluation a significant hurdle.

6.1.2 Optical Wireless Communications / Visible Light Communications

Regarding the VLC interface, we found no existing ns-3 modules capable of addressing the requirements for our project.

There is a solution available that combines VLC with Wi-Fi [110]. This module is noteworthy, as the authors validated their implementation using a real testbed and reported impressive results. However, when we attempted to use the publicly available code, we found it to be non-functional. After porting it to the latest version of ns-3 and solving different compilation errors, the implementation appears incomplete, making it impossible to reproduce the results described in the original research.

Nevertheless, the mathematical models presented in the study are quite valuable. Specifically, the authors provide a detailed mathematical model for the photo detector and represent light transmission using a Lambertian propagation loss model. However, the channel model does not account for ambient light interference, modeling a dark room environment. Moreover, the implementation of these models within the ns-3 framework revealed a critical limitation: the entire system was built on the point-to-point net device. This module, originally designed to simulate Ethernet communication between two nodes, severely constrained the flexibility and adaptability of the VLC implementation.

Figure 4 puts forward the architecture of this module. As we can observe, the structure of this model lacks a PHY layer and, consequently, a PHY state machine. Additionally, this module differentiates the TX from the RX by implementing them as two distinct classes. The TX Net Device is supposedly equipped with an LED for transmission, whereas the RX Net Device has a photo detector to receive the emitted signal. The opposite flow of traffic occurs from the point-to-point interface combining optical with radio. After further analysis, we understood the significant impact of this architecture on our ability to modify and expand the module. Ultimately, we determined that we needed to abandon this framework entirely and plan the development of a new module.

Our choice is to use the Simple Net Device in ns-3 as a foundation, which, as the name suggests, is a very basic model. This would allow us to implement components like an error model, integrate a mobility model, and start building a comprehensive physical layer, as well as a specific MAC layer if required.

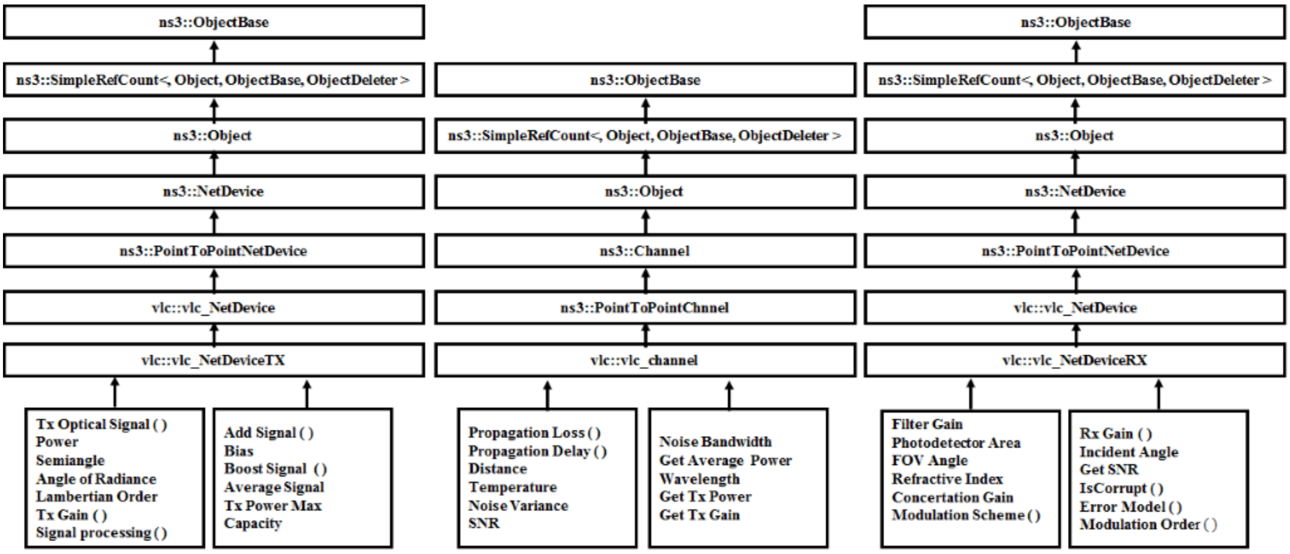

Figure 4: Structure of the state-of-the-art VLC module in ns-3 [111]

6.1.3 Energy Models

The ns-3 platform incorporates a versatile energy framework that serves as the foundation for modeling diverse energy consumption and harvesting scenarios [112]. The implementation of this framework was motivated by the emergence of energy technologies, such as fuel cells and energy scavenging. These energy solutions prove to be useful for low-power wireless devices, making ns-3 a robust candidate to develop the digital twin of the RIoT nodes. Figure 5 illustrates the energy framework implemented in ns-3, identifying its main modules organized in three primary categories: Source, Consumption, and Harvesting models.

- *Energy Source Models* – An energy source represents a power supply, powering every component installed on a given node. Upon complete depletion of the energy source, each interface is notified via its energy models, enabling them to shut down accordingly and turn on upon recharge. Additionally, each node has access to the energy source objects, providing crucial information such as remaining capacity, voltage, or state of charge. This accessibility facilitates the implementation of energy-aware protocols in ns-3. Related projects help to expand this versatility by developing energy models for different types of batteries or capacitors [113].
- *Energy Consumption Models* – The energy consumption models are associated with a specific communication module, monitoring its operation and consuming energy from the source according to its implementation. For example, the Wi-Fi Radio energy model defines a state machine to simulate the various PHY layer conditions: idle, CCA busy, TX, RX, channel switch, sleep, and off. Each state is linked to a specific current draw value in Amperes, from which the available energy can be updated or calculated.
- *EH Models* – Represents devices that supply energy from the environment to the energy source. These models include the complete implementation of the actual EH device (e.g., solar panel) and the environment (e.g., solar radiation), modeling both the environmental contribution and the device-specific factors. Unfortunately, as of the writing of this document, the harvesting mode can only be used with basic energy sources.

The energy consumption model of a device, designated as DeviceEnergyModel, is intended to be a state-based paradigm, where each device is assumed to have multiple states. Power consumption can be modeled as a lookup table, where each state is set to a constant current draw, but it can also integrate mathematical models defining current draw as a function of intrinsic parameters of the node.

The DeviceEnergyModel informs the associated EnergySourceModel of the device's updated power consumption whenever the state changes. The EnergySourceModel then updates the remaining energy and calculates the new total power consumption. A PHY listener facilitates communication between the device and the energy source. This class monitors the current PHY state of the device and notifies the source accordingly.

Since none of the existing ns-3 models, both BLE and VLC, integrate energy consumption models, there is an important need to develop dedicated energy models for each of these technologies. Implementing these models would involve defining the state machines for each communication module, mapping their operational states (e.g., idle, transmit, receive, sleep) to specific power consumption metrics. Additionally, these models must interface with the ns-3 energy framework to dynamically monitor and update the energy usage of the nodes during simulations.

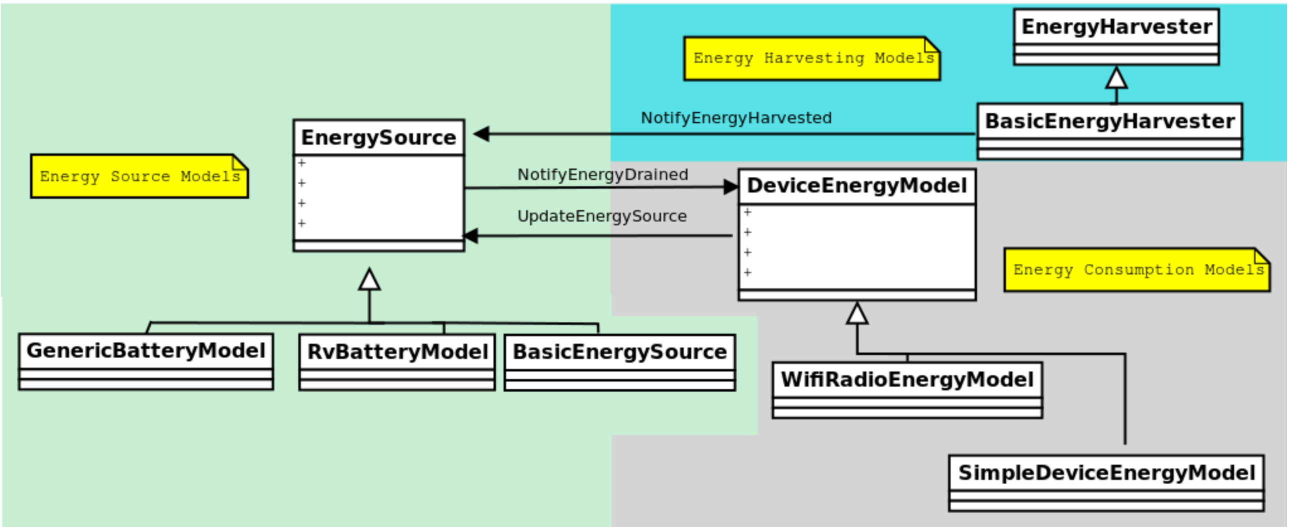

Figure 5: Energy Framework implemented in ns-3 [112].

6.2 ns-3 BLE – preliminary performance analysis

As stated previously, the BLE module was developed to attend the specific needs of the author and the BLE standard is not fully implemented. Therefore, due to the lack of documentation, it was a major challenge to reverse engineer the module, understand its limitations and fix existing issues to make it possible to analyse its performance. In this subsection, we conducted some tests to extract output metrics such as throughput and latency, while exploring different configuration scenarios, varying the distance between nodes, Connection Interval, Packet Size and other to identify the possibility of using these models and assess the potential performance of RIoT nodes and their potential for the target applications.

6.2.1 Link performance in a point-to-point connection

In our experiments testing the BLE state-of-the-art module, we began by assessing link performance in a simple point-to-point connection between two nodes. This setup aimed to uncover fundamental issues or flaws in the current state-of-the-art. Our findings showed that the module's performance was relatively unrealistic, primarily due to its implementation of the OQPSK modulation coding scheme. While this scheme delivers better results, it deviates from the standard GFSK, making the performance seem overly optimistic.

In Figure 6, we present a graph illustrating the illustrative link performance, with the signal-to-noise ratio (SNR) used as the performance metric. The graph shows that, as the distance between nodes increases from 20 centimeters to 100 meters, the SNR response remains remarkably strong. Comparing this to the bit error rate (BER), the OQPSK scheme also demonstrates significant resilience to noise. In Figure 7, we performed a simple verification to check if the TX power was properly implemented. The results confirm a direct linear relationship between TX power, ranging from -20 dBm to 20 dBm, and the observed SNR. Overall, these results indicate that, implementing the standard GFSK, which is known to provide higher performance than OQPSK, would provide a more realistic assessment of the module’s behavior.

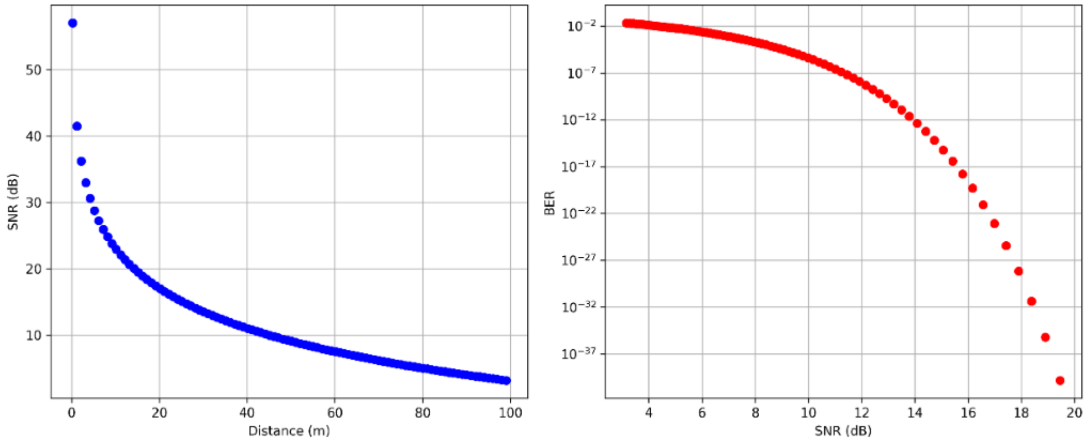

Figure 6: Performance of the BLE link. Left: SNR versus distance, showing the variation of SNR as the distance increases from 20 cm to 100 m. Right: Bit error rate versus SNR, illustrating the relationship between SNR and BER with the TX power fixed at 0 dBm.

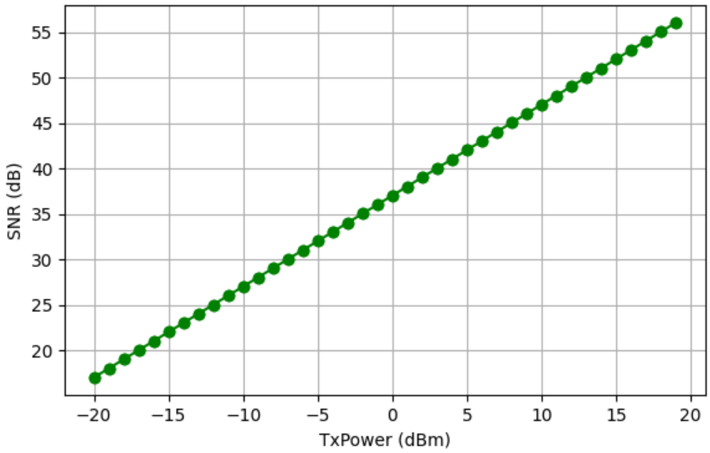

Figure 7: Verification of TX power implementation, showing the linear relationship between TX power (ranging from -20 dBm to 20 dBm) and the corresponding SNR at 2 m.

Continuing our analysis of link performance in a point-to-point BLE connection, we shifted our focus to throughput as the primary metric for evaluating performance quality. To enable monitoring of this metric, we designed a slightly more complex scenario, which required several adaptations to the BLE module. This was necessary because the module is not natively designed to integrate with ns-3 tools, such as Flow Monitor and other traffic generation applications, making it challenging to generate and monitor traffic effectively.

Our solution involved implementing User Datagram Protocol echo client-server connection. In this setup, the client sends a packet and waits for the server's response. To control the rate of application traffic generation, we adjusted the packet interval — a parameter that determines how frequently packets are generated. By decreasing the packet interval, we effectively increased the traffic generation rate. However, we identified a significant limitation: the packet interval was restricted to being at least twice the value of the connection interval — a configuration parameter of the BLE link. This restriction limited the flexibility of traffic generation. Additionally, we found that no more than one packet could be sent per connection interval. As a result, the observed throughputs were significantly lower than expected, highlighting a critical limitation in the module's design. These findings are represented in Figure 8. The plot clearly shows the limited throughput, with a maximum of only 16 kbit/s, confirming the constraints imposed by the BLE module.

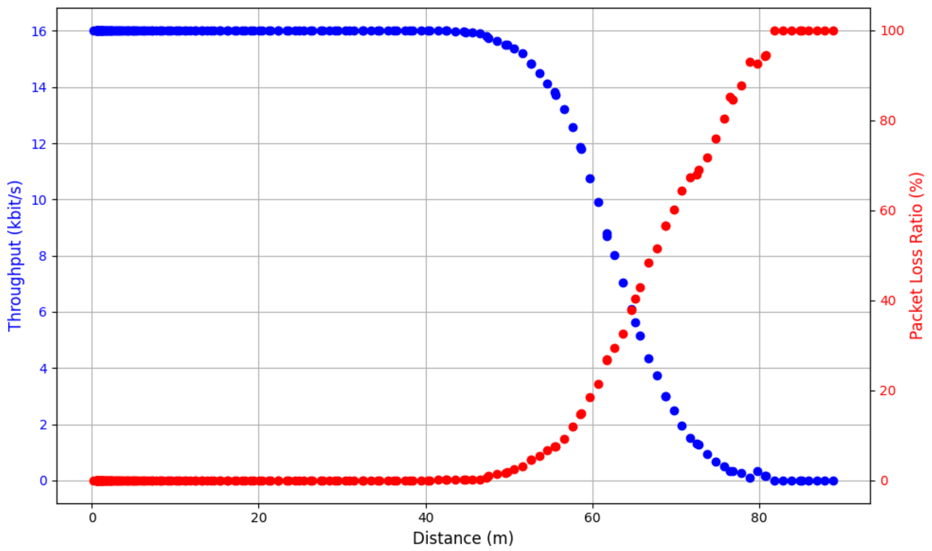

Figure 8: Throughput and packet loss variation over distance in the BLE link for 0 dBm.

To improve throughput, we experimented with adjusting both the connection interval and packet size to optimize performance. With a packet size of 27 bytes, the best throughput we could achieve was 16 kbit/s. We also varied the connection interval, as shown in Figure 9, testing values from 6 (7.5 ms) up to 20 (25 ms). However, we found that a connection was only established for connection intervals of 11 (13.75 ms) or higher. Below this value, no traffic occurred, limiting our throughput to 16 kbit/s. Furthermore, the plot shows that as the connection interval increases, the throughput diminishes and latency increases, further demonstrating the trade-off between connection interval and performance.

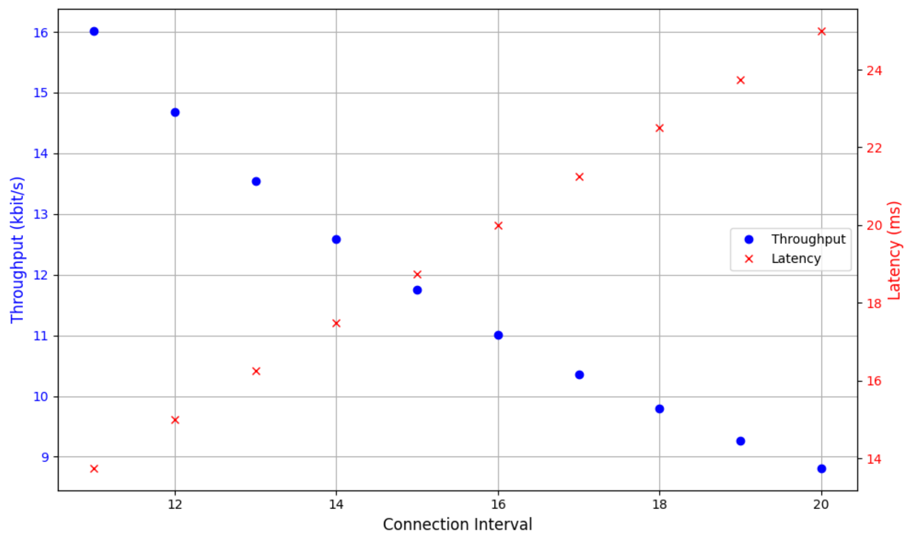

Figure 9: Throughput and latency variation over different connection intervals (*ConnectionInterval* per BLE specification are denoted in 1.25 ms units)

Moving on to the next experiment, we explored how varying the packet size could improve throughput. We tested packet sizes ranging from as low as 27 bytes to as high as 200 bytes, and we observed a clear increase in throughput with larger packet sizes, as shown in Figure 10. However, while this does improve throughput, we are still limited by the maximum packet size of 200 bytes. This limitation persists since the packet size is limited to 251 bytes (considering LE Data Length Extension enabled) by the standard. This remains a significant issue that needs to be addressed, and the experiment serves as another way of highlighting this limitation.

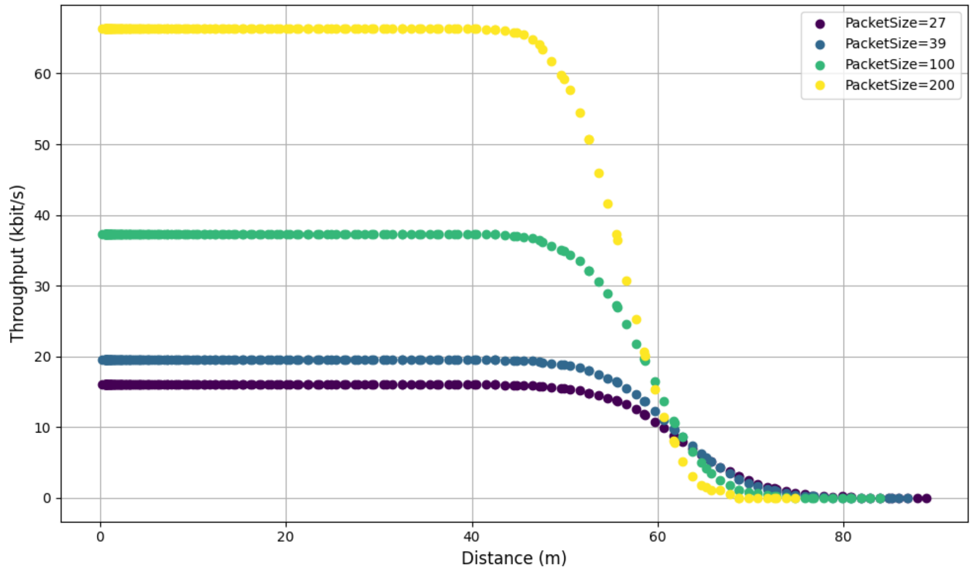

Figure 10: Throughput variation over distance for different packet sizes in the BLE link at 0 dBm.

6.2.2 Mesh network support and link performance vs. number of hops

When it comes to measuring the link performance in a possible mesh network, the throughput was tested across a varying range of connection intervals and with an increasing number of hops with nodes placed in a line at a distance of 15 m apart. As is shown in Figure 11, a decrease in throughput is initially observed as the number of hops increases. However, the throughput rises when 5 hops are reached. This measuring error may be due to the incompatibility of the state-of-the-art model with common ns-3 applications used to measure throughput, thus causing inaccuracies. This shows the state-of-the-art model does not correctly support mesh networks and is a limitation.

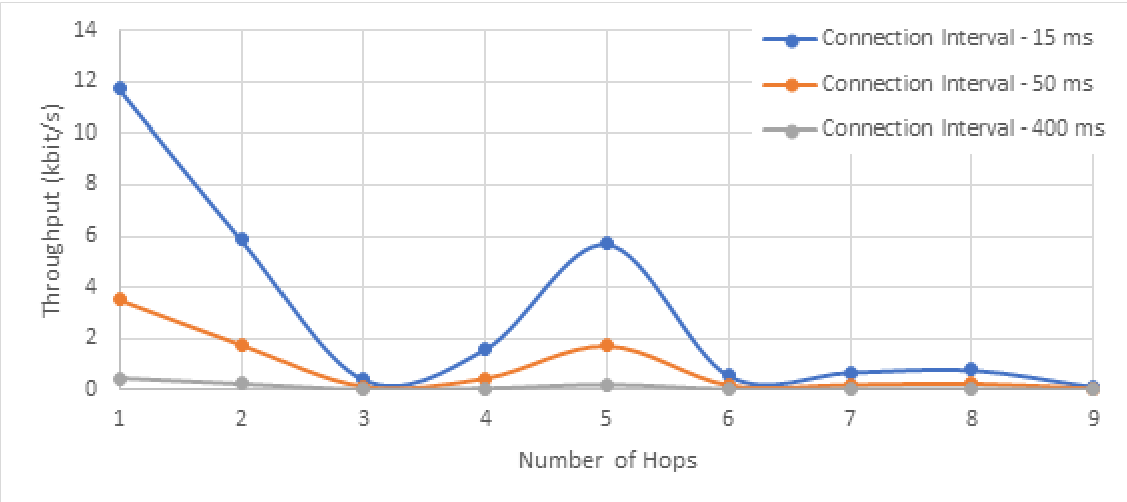

Figure 11: Throughput variation over number of hops for different connection intervals in the BLE link.

6.3 Summary

6.3.1 Main conclusions

Our preliminary study on the state-of-the-art ns-3 modules was crucial in identifying key issues and limitations within these solutions. Despite limited documentation for the respective modules, our research involved a hands-on assessment of the functionality and specifications of both the BLE and VLC ns-3 modules.

The findings revealed that no existing work directly supports the VLC module, necessitating its implementation from scratch. For BLE, the current module is still significantly underdeveloped, lacking the maturity needed to simulate the network topologies and scenarios relevant to this project. Key shortcomings include incompatibility with existing ns-3 tools, limited analytical capabilities, and, most of all, inadequate flexibility to implement scenarios outside the original author's intended use.

6.3.2 Known limitations

As for the main limitations, it has already been possible to critically identify the main problems of the BLE module, including:

- *Absence of Modern PHY Features* – The current implementation does not support the modern 2M PHY layer.
- *Non-Standard Modulation Coding Scheme* – The module employs a non-standard modulation coding scheme, deviating from established BLE specifications.
- *Partial BLE Standard Implementation* – Only a subset of the BLE standard has been implemented, leaving significant features unaddressed.
- *Functional Limitations* – Certain features are only partially operational; for example, only one packet can be sent per connection interval.
- *Compatibility Issues* – The module lacks compatibility with existing ns-3 tools, hindering integration with broader simulation frameworks.
- *Restricted Scenario Flexibility* – Limited options for configuring network topologies or scenarios, constraining its applicability to diverse use cases.

Regarding the VLC module, the publicly available code is not functional and due to its fundamental architectural restrictions, the development of a new module from scratch is necessary. Additionally, both models require the implementation of a dedicated energy consumption model.

6.3.3 Next steps

Considering these constraints, our attention will have to be divided into BLE and VLC modules, focusing on mitigating the shortcomings of the BLE, and implementing the VLC module from scratch. Eventually, when both technologies are mature enough, they will be integrated into the same node, which will be achieved by creating a dedicated ns-3 module for the RIoT nodes. In future work, we plan to implement the following features:

- Bluetooth Low Energy ns-3 module:
  - GFSK modulation coding scheme error model
  - PHY 2M, adding support for 2 Mbit/s bitrate
  - Develop new BLE applications, allowing for different network topologies and compatibility with ns-3 tools
  - Develop a dedicated energy consumption model
- Visible Light Communication ns-3 module:

  - Design and implement the ns-3 models for photodetector and optical transceivers
  - Implement a PHY layer model for the optical interface
  - Develop the optical channel model and propagation loss model for infrared and visible light
  - Develop a dedicated energy consumption model
- RIoT ns-3 module:
  - Integrate both interfaces into a single node
  - Define a gateway and end node variation of the nodes
  - Elaborate a star topology scenario
  - Perform energy consumption simulations

The progress on network simulation tool development and employing them for performance analysis beyond D3.1 will be reported in D3.4 and other project deliverables.

7 Alignment with the 6G SNS and roadmap

Though preceding it by around 1 year, the SUPERIOT network architecture is well-aligned with the 6G-IA and 6GSNS design principles and network architecture reported and detailed, e.g., in [114]-[116] and depicted in Figure 12. Notably, the SUPERIOT architecture is built based on the same principles ([116] p. 22) including (i) exposure of capabilities, (ii) extensibility and flexibility, (iii) scalability, (iv) resilience and availability, (v) service-based interface, (vi) separation of network functions and (vii) network simplification.

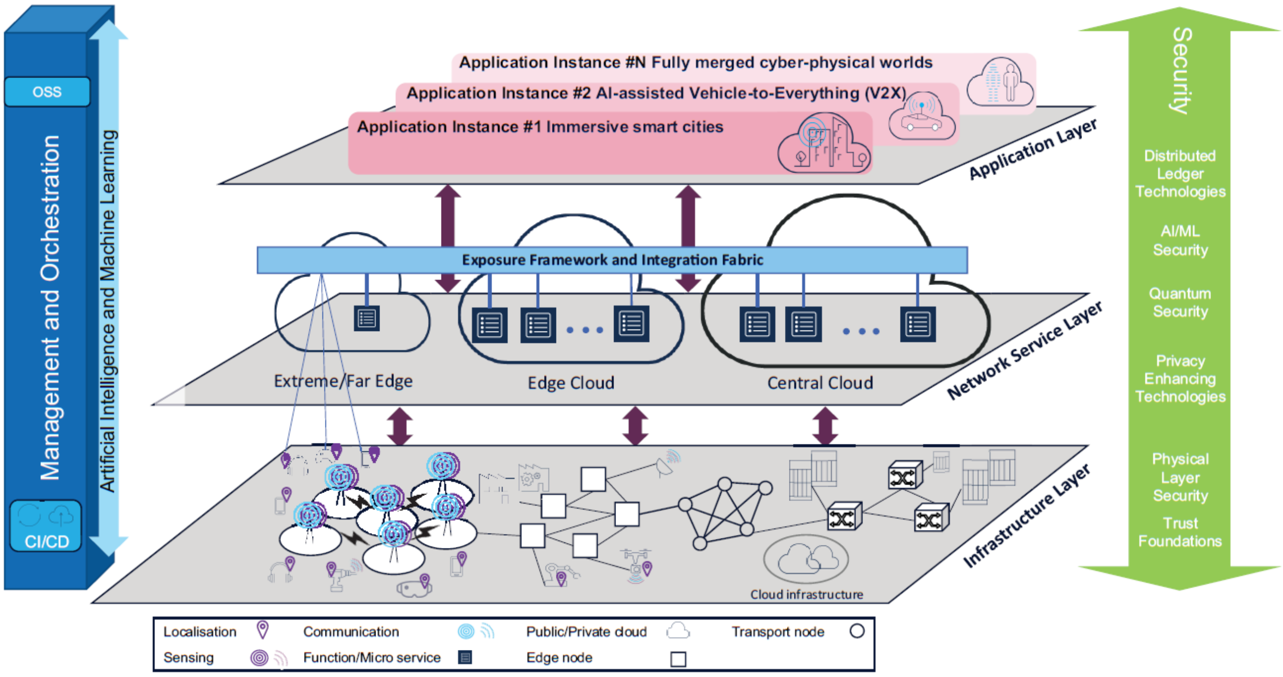

Figure 12: End-to-end system view of the 6G architecture by 6G SNS (reprinted from [114]-[116]).

Comparing Figure 12 with SUPERIOT architecture presented in Figure 2 several observations can be made:

- The 6G-IA and 6GSNS network architecture is more comprehensive and details the network service layer and applications, which are not explicitly detailed for SUPERIOT architecture, given that our project focuses primarily on the IoT device production technologies and physical and link layers of the communication (and beyond communication – i.e., localization and power supply) stack. Nonetheless, the service/microservice-based architecture utilized by the 6G SNS (and employed in cellular networks since their fifth generation – 5G [117]) is also selected as the basis of the SUPERIOT network architecture; this decision was made to boost its flexibility, scalability and resilience. However, given the limited volume of the SUPERIOT project and the needs of our target applications, the number of network services will be substantially reduced to effectively demonstrate the key features of SUPERIOT technologies (i.e., dual mode communication and localization and their optimizations). For instance, the functions dealing with billing and policy control will be out of the scope of our development and implementation. Similarly, considering the focus of the project, the interfaces between the different network architecture elements will be simplified by using well-established technologies (e.g., the MQ Telemetry Transport service and JavaScript Object Notation).
- It can be noted that the network presented in Figure 2 focuses primarily on conventional human user terminals; the functionality of the network is limited to communication and sensing (while localization can be treated as a subcase for sensing). Meanwhile, the foreseen SUPERIOT architecture focuses on IoT devices, and thus, its functionality is more

diverse and includes the possibility of powering the RIoT nodes in addition to enabling their communication and positioning. This requires more flexibility from our base stations/APs (e.g., support of standalone power supply APs – "power beacons", or APs providing only localization service), which must also be supported by the overall network architecture. Similarly, integration of RIS as a part of the network infrastructure to support the most limited IoT nodes, calls for a more flexible approach and development of the appropriate RIS control interfaces.

– The advanced computing services (e.g., edge and cloud computing) and AI/ML support, though not being in the direct focus of the SUPERIOT project, are important aspects of the next-generation IoT services and, due to the service-based approach taken, can be seamlessly integrated into the SUPERIOT architecture in the future.

When this comes to the alignment with the 6GSNS timeline (refer to slide 7 in [116]), the SUPERIOT architecture, though not directly compatible with cellular network architecture as its radio layer bases on a non-3GPP technology, can offer relevant insights towards the future development of the harmonized 6G network architecture, particularly focusing on the use of VLC/hybrid RF-VLC, and efficient integration of fully passive and ultra-low consuming IoT terminals and the required for their support infrastructure elements into the 6G networks of the future.

Notably, departing from the overall network architecture specification presented in this document, the SUPERIOT will further detail the architecture (e.g., by specifying the network services structure and respective interfaces) in the follow-up documents and demonstrate them as a part of milestone 4.

8 Gateway and embedded PC specification

In the previous section, the overall architecture of the SUPERIOT network has been sketched. In the current section, we focus specifically on the AP/gateway and embedded PC, which are the elements of the SUPERIOT network closest to the end nodes. In the following sections, we discuss and list the design details and requirements for the gateway. It is worth noting that to achieve the target of the overall sustainability of the SUPERIOT solution (quantification methodology for which is being developed by Task 1.4), two critical aspects have to be considered at the network and system levels. First, likewise for the SUPERIOT RIoT node, the sustainability of production processes and procedures related to network infrastructure. Therefore, we expect that some methods, technologies and designs developed (e.g., printed electronics) for RIoT node in the context of SUPERIOT WP2 can also be employed in WP3. Second, ensuring the efficiency of the overall operations of the SUPERIOT network as a whole is of paramount importance. To this end, task 3.4 of WP3 will look into this challenge by developing relevant optimisation methods.

8.1 Gateway and embedded PC for communication service(s)

The gateway considered in the SUPERIOT project has either an RF front-end, optical front-end, or both, providing connectivity and, potentially, other services to the RIoT nodes. In general, the gateway offers wireless connectivity to the RIoT nodes. It gets/forwards the data from/to the embedded PC, which manages multiple gateways as shown in Figure 13 (refer also to the overall network structure depicted in Figure 2).

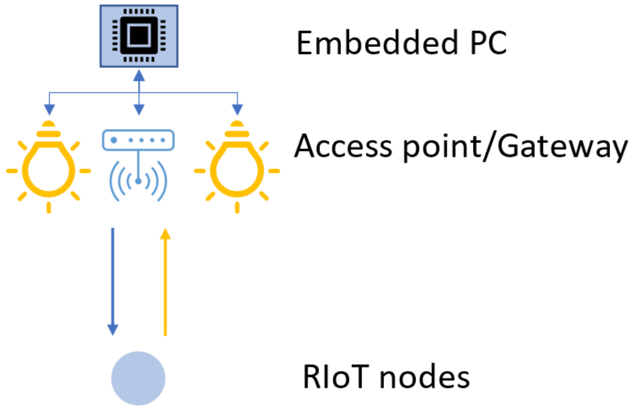

Figure 13: The gateway is the main link between RIoT nodes and the embedded PC or the main server.

8.1.1 Companion embedded PC

The embedded PC comprises single-board computers, with its main distinguishing features being low energy consumption and ease of implementation and set-up. Although embedded PCs' tasks are limited in terms of computational demand, they should be nonetheless able to run simple signal processes and potentially also run artificial intelligence (AI)-based algorithms. The main role they play, from the communication point of view, is to handle the MAC layer and process channel measurements, if any are needed. In the SUPERIOT project, we will explore two types of embedded PC: the Raspberry Pi (as the primary option) and the BBB microcontroller (as a secondary option).

Model 4B has been selected for a Raspberry Pi, which is the latest release. Its controllers have a Quad-core Cortex-A72 (Advanced Reduced Instruction Set Computer (RISC) Machines (ARM) v8) 64-bit SoC, 4 GB of random access memory (RAM), and multiple input/output (I/O) connections such as USB C, USB 3.0, and a 40-pin general purpose input-output (GPIO) header. The single-board computers are connected to the server and to the Internet using either Ethernet or Wi-Fi. The former interface will be used as the baseline, while the latter can be employed for demonstration and field tests requiring a higher degree of mobility.

In the case of the BBB, the board runs a Debian Linux distribution. It has a 32-bit ARM Cortex A8 with a clock frequency of 1 GHz, 4 GB of flash memory and 512 MB of RAM. The board also has 2 Programmable Real-time Units (PRUs) running at 200 MHz, providing real-time processing capabilities typically missing in Linux operating systems. Further, the board has 65 digital inputs/outputs and seven analogue inputs to interface with external devices. The baseline version has an Ethernet connection for interconnection with other boards. The BBB Wireless variant, which is used for the processing units of the RXs, is equipped with WiFi.

8.1.2 Gateway

As shown in Figure 13, the AP in the SUPERIOT project supports either RF, optical, or both. For RF connectivity, we consider BLE one of the most popular IoT communication technologies. It uses an unlicensed spectrum, and it was released to extend Bluetooth applications to IoT sensors, wearables, and to other devices with low energy consumption requirements, making it a perfect fit for the SUPERIOT scenarios. Moreover, the BLE Mesh variant can be exploited, thus enabling multi-hop wireless communication schemes to surpass the number of devices and coverage limitations imposed in regular BLE networks.

A popular off-the-shelf silicon-based hardware for BLE is the Nordic Semiconductors nRF52DK development kit, which can act as the gateway, a.k.a master node in the BLE standard [118]. The board is powered by the c low-power System on Chip (SoC), which is built on an Arm Cortex M4 Central Processing Unit (CPU) with a floating point unit running at 64 MHz, which is capable of efficient processing with a very low voltage supply and power consumption [119]. For instance, it can be powered from a coin cell battery CR2032 and features 32 GPIO pins and wireless connectivity using BLE, BLE Mesh, and Near Field Communications (NFC). Notably, the SoCs of the same producer and belonging to the same family will be used by RIoT nodes (the Si-based reference node design, at minimum) [2]. This ensures compatibility between and supports and facilitates re-using the code between the RIoT nodes and the gateway.

In the case of the optical gateway, the core element is the LED itself, which represents the front end. In particular, in the SUPERIOT project, we consider a CREE XT-E LED and the companion hardware circuitry to modulate the intensity of the light signals. Different designs of the LED front end are possible, ranging from the ones with a simplistic circuit where the signal modulating an optical waveform comes from a GPIO line of the companion PC and up to more sophisticated designs, including a (micro)controller responsible for optical modulation and having a serial interface to the companion PC. Both options can be implemented within one board to enable higher flexibility for the future. Overall, the LED front-end has two operating modes: illumination mode and illumination plus communication mode.

- Illumination mode: The LED is solely used for illumination in this mode, which is achieved by applying a constant bias current that is close to its nominal drive current. This mode is particularly interesting for the case where the LED is used as an energy source for the RIoT nodes.
- Illumination plus communication mode: In this mode, the light intensity emitted from the LED is modulated to transmit data using a modified OOK, where a swing level around the bias is adopted to distinguish the symbols HIGH and LOW.

8.2 Gateway and embedded PC for localization service(s)

This section discusses the design details and requirements of the gateway for localization services. The AP in the SUPERIOT project supports either RF, optical, or both, as demonstrated in Figure 2. Based on our current knowledge, we consider that the gateway for the localization system will employ the functionalities and will be integrated with communication architecture.

In recent years, various RF wireless technologies have been studied for localization. Particularly, WLAN technology is widely used for wireless communication. In a Wi-Fi localization system, the target can only be a wireless terminal; thus, it is unsuitable for the case with low energy constraints. UWB technology can provide high position accuracy, but the UWB localization system requires a wide spectrum and high construction costs. On the other hand, BLE technology is widely used in IoT applications to enable communication between different devices while offering low cost and power consumption. Thus, we believe BLE is the most promising technology for RF-based localization. There are also new upcoming features of BLE, such as electric shell label and channel sounding, which are expected to provide improved ranging based on a PDOA. As mentioned earlier, the widely used commercially off-the-shelf hardware for BLE is the Nordic Semiconductors nRF52DK. It is powered with a CR2032 battery and provides BLE, BLE Mesh and NFC for wireless connectivity. All these functionalities can be employed for implementing localization.

In addition, RFID technology can be another promising candidate as it plays a key role in the IoT concept. Passive RFID tags are expected to replace conventional barcodes and become the main logistics and item management technology. RFID localization system can locate and identify the object while being suitable for scenarios with long-range and low power constraints requirements. Therefore, we believe RFID technology has a promising aspect for localizing sustainable IoT, making it ideal for some SUPERIOT applications. In the literature, RFID reader RRU4500 from Katherien Solutions with WRA7070 and MIRA-100 antenna types are used; however, accessibility to the specification of those is limited. Alternatively, the SDR is utilized and programmed as an RFID reader. We consider SDR as a suitable option, where SDR will be connected to a PC via Ethernet and on the PC, some algorithms can be implemented to control the EPC-compliant reader. Among the various SDRs, the Ettus N210 with the SBX daughter board is used due to the accessibility of the schematics and the high sampling rate. Traditional RFID tags operate at 860-960 MHz narrowband. On the other hand, the dual-frequency band NXP Semiconductor UCODE 7 EPC tag can perform at both conventional bands and 2.45 GHz, which is compatible with BLE technology. Such tags can use EPC Gen2 standard arbitration protocol for identification purposes and use 2.45 GHz for localization purposes. For the antennas, Huber&Suhner SPA-2400/75/0/V antenna can be selected for 2.45 GHz, and Huber&Suhner SPA-8090/78/8/0/V antenna model can be used for the ultra-high frequency bands.

For the VLP localization system, we consider the RSS-based approach. The main advantage of the R.SS-based method is that it can be employed with a photodiode RX, which makes it a perfect fit for semi-printed and fully printed IoT cases, and thus we believe it is a promising candidate for localization in sustainable IoT concept. Moreover, RSS-based VLP can cooperate with the existing communication network architecture, and it does not require anything hardware-wise beyond what is already needed for VLC.

8.3 Gateway and embedded PC for energy transfer service(s)

Following the discussion in Section 5.4.3, SWIPT and SLIPT will be implemented using the hardware and software components implementing the communication service (discussed in Section 8.1), with some modifications if required.

Specifically, the wireless energy transfer over both optical and RF is as follows:

- The illumination mode of the optical communication gateway's front end will be employed for light-based energy transfer, as discussed in Section 8.1. If necessary, modifications to the design of the optical front end will be introduced to increase the dynamic range of the radiated light's intensity. Various filters to experiment with polarized light or filter particular wavelengths might also be introduced. Also, various lenses can be trialled to experiment with the different beam widths. Adding optical communication functionality to the gateway will increase power consumption. This is called a power penalty when communication is added on top of illumination mode [98]. Here, the expectation is to have a maximum of 50% more power consumption, but that depends on the LED type, the implementation of the hardware (the data driver), and the data rate intended to be used. This extra energy consumption at the gateway does not reflect in EH on the node. The measured EH using an OPV with only illumination and illumination plus communication is depicted in Figure 14.

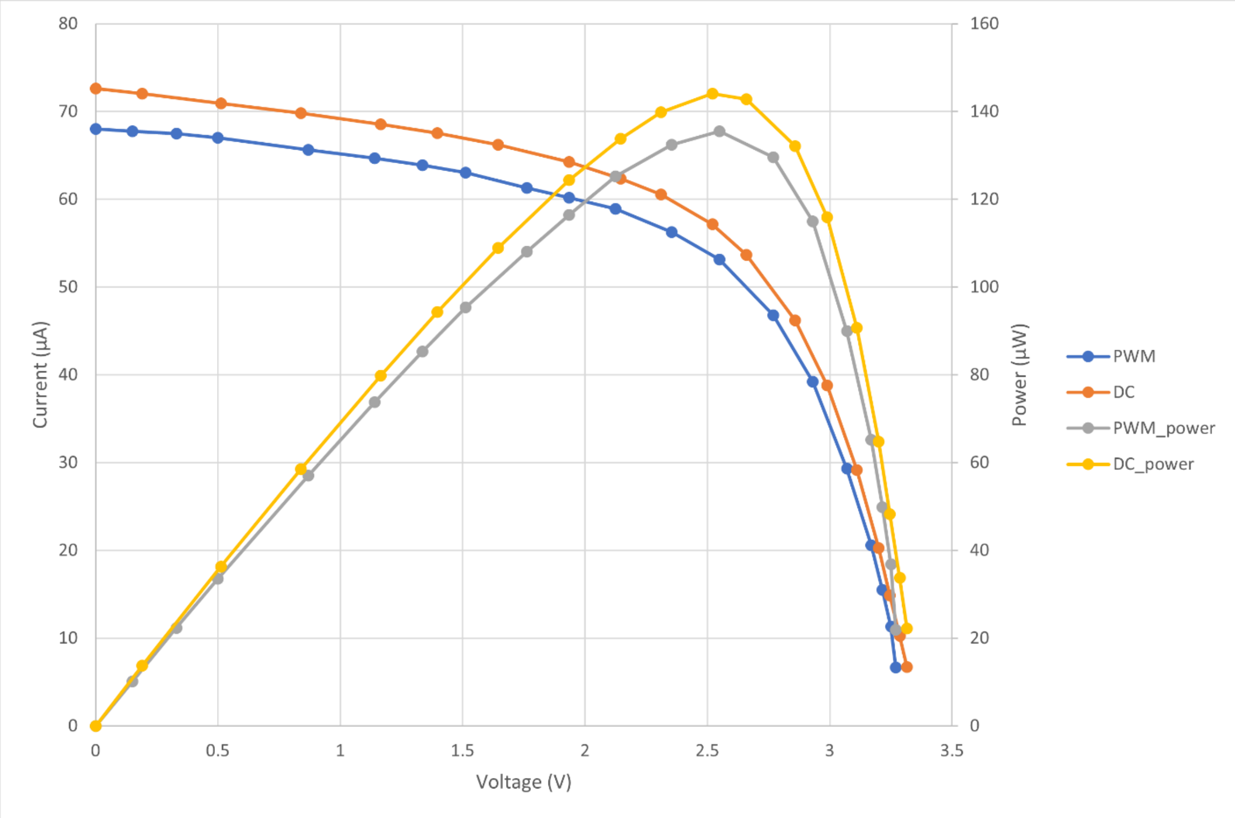

Figure 14: Measured harvested energy for DC illumination standalone, and DC illumination with added communication functionality. The measurement is conducted using a white LED, with both DC (illumination) and communication (PWM) power consumption maintained at 2 W, producing 800 lx and 750 lx, respectively. Despite the same power consumption, a light intensity difference of approximately 6.5% led to around 6% variation in the harvested power.

The radio module based on nRF52DK will be employed for RF-based energy transfer. Similar to optical communication and energy transfer, two different modes of RF energy transfer will be considered. The former implies that RIoT nodes harvest energy from conventional BLE packets. The latter option implies transmitting specialized signals (e.g., a carrier wave or a sweep waveform) that carry the energy from the AP to the RIoT nodes. Such signals will be generated using, e.g., the radio test functionality of the BLE SoCs and the respective code examples [120]. Considering RF attenuation, the GW to be used as RF energy TXs can be equipped with an external power amplifier, which will be connected to the MM8130-2600 antenna connector of the development board along with an external antenna (either an omnidirectional or a directive one). Given the limited power budget of the radio board, an external DC power supply will be required to power the amplifier. Depending on the target of the experiments, either an amplifier with a fixed or variable gain can be employed. If simultaneous communication and energy transfer are required, a single embedded PC can be instrumented with two RF boards – one implementing communication service and another transmitting energy. The RF functionality, if it is used for communication or EH, does not add extra power consumption on the gateway. The gateway does not need an extra driver to perform data communication. Hence, no extra power penalty is foreseen at the RF gateway. No need for hardware modifications for the embedded PC for implementing energy transfer functionality is expected.

8.4 Integration

The discussion in Sections 8.1-8.3 shows that the implementation of the three considered functionalities is majorly based on the same components, which facilitates and supports their integration. Notably, the availability of the multiple interfaces (at least 4 USB and 2 UARTS; the USB ports can be further split using a USB hub and/or extend the number of available UART ports or GPIOs by using, e.g., FTDI UART-USB converter chips if required). The specialized (i.e., implying substantial hardware modifications to the baseline optical and RF boards, which implement the basic communication functionality) versions of optical and RF boards (e.g., containing an SDR or RFID TX) will be instrumented following a modular approach and aiming to support their hardware compatibility with the baseline boards, whenever possible. This approach will ensure high flexibility of the developed system and contribute to reaching overall sustainability. Additionally, whenever feasible, the connectors should enable support for controlling the power supply and measuring the energy consumption of the individual components of the gateway (e.g., radio/optical transceivers, processing unit).

9 Conclusions

This deliverable focused on the SUPERIOT network architecture and specified the design of the SUPERIOT gateway. We started by defining the network architecture notation and identifying the elements of the network architecture. Then, we briefly presented and discussed the state of the art for the identified elements. Next, we departed from the results of the potential SUPERIOT application definition work, executed by SUPERIOT WP1 and reported in deliverable D1.1 document, to specify the functionalities that have to be implemented by a SUPERIOT network and which affect the design of the network architecture. Specifically, we have identified three main functionalities that the network must support. These are:

- wireless connectivity,
- localization,
- and wireless energy transfer.

Notably, while the two formers are required for many of the potential SUPERIOT applications and use cases and thus can be considered obligatory, wireless energy transfer is not mandatory, especially if the energy necessary for the operation of RIoT nodes can be collected from ambient sources. Nonetheless, the support of purposeful energy transmission from SUPERIOT network infrastructure to RIoT nodes can substantially increase the reliability of the overall system's operation. For this reason, we discussed the means and are planning to implement some support for this functionality. We analysed the application requirements for each of the three identified functionalities, discussed the state-of-the-art and sketched the potential network architecture. Also, we highlighted the interrelation between these three functionalities and discussed how they can be integrated to form a multifunctional network based on multi-modal radio-optic SUPERIOT connectivity.

Specifically, a five-tier network architecture topology is planned for the SUPERIOT network composed of (from bottom to top):

- the RIoT nodes,
- the gateways/AP implementing visible light and/or RF connectivity and/or localization and/or energy transfer,
- the embedded PCs controlling and providing backbone connectivity for gateways/APs,
- a network switch(es) enabling Internet or local network access for embedded PCs,
- a central (cloud) server controlling the whole SUPERIOT network and implementing required applications.

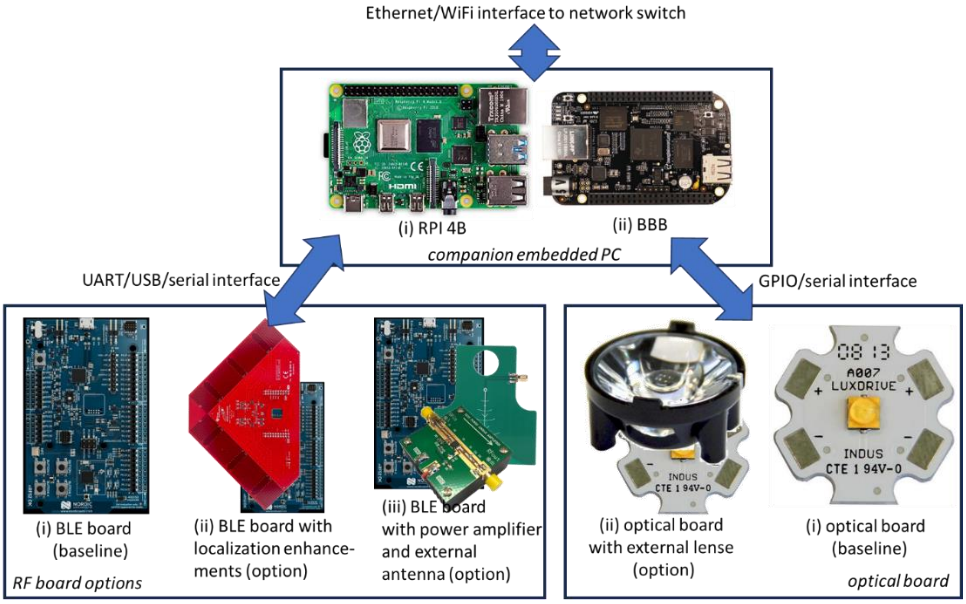

Figure 15: Structure of the envisaged SUPERIOT gateway and companion embedded PC.

Table 8. The key elements of the SUPERIOT access point and embedded PC (baseline version).

Component	Key hardware element (s)	Notes and comments
Embedded PC	Raspberry Pi Model 4B and BEAGL-BONE-BLACK	Raspberry Pi Model 4B is the primary platform, BEAGL-BONE-BLACK is the secondary; software based on respective Linux distributives.
Radio board	nRF52DK	
Optical board	The electronic board based on CREE XT-E LED	

Next, we specified the architecture of the SUPERIOT gateway and companion embedded PC. Its envisaged structure and key components are illustrated in Figure 15 and listed in Table 8. A companion embedded PC is interfaced to one or multiple RF and/or optical boards implementing the desired set of functionalities. Modified and more specialised designs can be employed for some experiments and proofs-of-concept instead (or in addition to) the baseline RF/optical boards. In these cases, the interface of the modified boards will be kept as much similar to the baseline board as possible. However, additional control interfaces (e.g., based on GPIOs or serial interfaces) can be introduced to control the newly-added functionalities. To facilitate the integration of the different functionalities, the modified boards should be, whenever possible, designed in such a way as to enable their parallel usage with the baseline boards. Notably, the selection of the hardware components composing the SUPERIOT gateway was aligned with that to be used by the SUPERIOT RIoT node, thus facilitating and enabling the re-use of hardware designs and software codes and contributing to reaching the goal of higher overall sustainability of IoT solutions, manifested by the SUPERIOT project.

This deliverable establishes the basis for the further design and optimization of the SUPERIOT network and the individual functionalities to be supported by it. As such, the document will be used by all subtasks in WP3 and reveal the planned network architecture for other WPs of the project (especially WP2 and WP4). The discussion of the technical state-of-the-art and analysis of the application requirements provided in this document can also be helpful for WP1 in assessing the feasibility and potential of the different applications and/or demonstrations. In the follow-up work, we will focus on specifying the interfaces between the different components further and characterizing the sustainability of the planned architectures once the respective methodology is developed by SUPERIOT task 1.4.

10 Bibliography

[1] SUPERIOT HORIZON-JU-SNS-2022 project no 101096021, "D1.1 Description of selected scenarios, applications, and their requirements," version 1.0, March 2023.

[2] SUPERIOT HORIZON-JU-SNS-2022 project no 101096021, "D2.1 Node architecture," version 0.1, August 2023.

[3] V. Kanade, "What Is Network Hardware? Definition, Architecture, Challenges, and Best Practices," available online (1.5.2023): https://www.spiceworks.com/tech/networking/articles/what-is-network-hardware/

[4] IBM, "What is networking?," available online (1.5.2023): https://www.ibm.com/topics/networking

[5] N. Cen, J. Jagannath, S. Moretti, Z. Guan, and T. Melodia, "LANET: Visible-light ad hoc networks," Ad Hoc Networks, vol. 84, pp. 107–123, Mar. 2019, doi: 10.1016/j.adhoc.2018.04.009.

[6] M. Obeed, A. M. Salhab, M.-S. Alouini, and S. A. Zummo, "On Optimizing VLC Networks for Downlink Multi-User Transmission: A Survey," IEEE Communications Surveys & Tutorials, vol. 21, no. 3, pp. 2947–2976, 2019, doi: 10.1109/COMST.2019.2906225.

[7] H. Abuella et al., "Hybrid RF/VLC Systems: A Comprehensive Survey on Network Topologies, Performance Analyses, Applications, and Future Directions," IEEE Access, vol. 9, pp. 160402–160436, 2021, doi: 10.1109/ACCESS.2021.3129154.

[8] A. Al Hammadi, P. C. Sofotasios, S. Muhaidat, M. Al-Qutayri, and H. Elgala, "Non-Orthogonal Multiple Access for Hybrid VLC-RF Networks With Imperfect Channel State Information," IEEE Transactions on Vehicular Technology, vol. 70, no. 1, pp. 398–411, Jan. 2021, doi: 10.1109/TVT.2020.3044837.

[9] F. Wu, L. Chen, and W. Wang, "HRO-OFDM Scheme Design and Optimization for a Hybrid RF/VLC Baseband System," IEEE Photonics Journal, vol. 9, no. 5, pp. 1–13, Oct. 2017, doi: 10.1109/JPHOT.2017.2728102.

[10] V. K. Papanikolaou, P. D. Diamantoulakis, and G. K. Karagiannidis, "User Grouping for Hybrid VLC/RF Networks With NOMA: A Coalitional Game Approach," IEEE Access, vol. 7, pp. 103299–103309, 2019, doi: 10.1109/ACCESS.2019.2930169.

[11] M. Goldwater et al., "An 802.11 Compatible Asymmetric Hybrid Visible-Light and Radio-Frequency Communications System," in Proc. IEEE 31st Annual International Symposium on Personal, Indoor and Mobile Radio Communications, Aug. 2020, pp. 1–7. doi: 10.1109/PIMRC48278.2020.9217371.

[12] R. P. Naik and W. -Y. Chung, "Evaluation of Reconfigurable Intelligent Surface-Assisted Underwater Wireless Optical Communication System," in Journal of Lightwave Technology, vol. 40, no. 13, pp. 4257-4267, 1 July1, 2022, doi: 10.1109/JLT.2022.3162627.

[13] A. R. Ndjiongue, T. M. N. Ngatched, O. A. Dobre and H. Haas, "Digital RIS (DRIS): The Future of Digital Beam Management in RIS-Assisted OWC Systems," in Journal of Lightwave Technology, vol. 40, no. 16, pp. 5597-5604, 15 Aug.15, 2022, doi: 10.1109/JLT.2022.3176762.

[14] W. Zhang, X. Zhao, and G. Jiang, "Physical Layer Security for Intelligent Reflecting Surface-Assisted VLC/RF Hybrid Network," in Proc. 14th International Conference on Communication Software and Networks, Jun. 2022, pp. 23–27. doi: 10.1109/ICCSN55126.2022.9817602.

[15] A. Almehdhar, M. Obeed, A. Chaaban, and S. Zummo, "A Hybrid VLC/RF Cell-Free Massive MIMO System," in Proc. IEEE International Conference on Communications, May 2022, pp. 1871–1876. doi: 10.1109/ICC45855.2022.9838980.

[16] Y. Xiao, P. D. Diamantoulakis, Z. Fang, L. Hao, Z. Ma, and G. K. Karagiannidis, "Cooperative Hybrid VLC/RF Systems With SLIPT," IEEE Transactions on Communications, vol. 69, no. 4, pp. 2532–2545, Apr. 2021, doi: 10.1109/TCOMM.2021.3051908.

[17] T. Rakia, H.-C. Yang, F. Gebali, and M.-S. Alouini, "Dual-Hop VLC/RF Transmission System with Energy Harvesting Relay under Delay Constraint," in Proc. IEEE Global Communications Conference Workshops, Dec. 2016, pp. 1–6. doi: 10.1109/GLOCOMW.2016.7848882.

[18] G. Pan, H. Lei, Z. Ding, and Q. Ni, "On 3-D Hybrid VLC-RF Systems with Light Energy Harvesting and OMA Scheme over RF Links," in Proc. IEEE Global Communications Conference, Dec. 2017, pp. 1–6. doi: 10.1109/GLOCOM.2017.8254799.

[19] M. R. Zenaidi, Z. Rezki, M. Abdallah, K. A. Qaraqe, and M.-S. Alouini, “Achievable Rate-Region of VLC/RF Communications with an Energy Harvesting Relay,” in Proc. IEEE Global Communications Conference, Dec. 2017, pp. 1–7. doi: 10.1109/GLOCOM.2017.8254192.

[20] J. Chen and Z. Wang, “Topology Control in Hybrid VLC/RF Vehicular Ad-Hoc Network,” IEEE Transactions on Wireless Communications, vol. 19, no. 3, pp. 1965–1976, Mar. 2020, doi: 10.1109/TWC.2019.2960229.

[21] J. Chen and Z. Wang, “Coordination Game Theory-Based Adaptive Topology Control for Hybrid VLC/RF VANET,” IEEE Transactions on Communications, vol. 69, no. 8, pp. 5312–5324, Aug. 2021, doi: 10.1109/TCOMM.2021.3077950.

[22] S. Ghosh and M.-S. Alouini, “On the Performance Optimization of Two-Way Hybrid VLC/RF-Based IoT System Over Cellular Spectrum,” IEEE Internet of Things Journal, vol. 9, no. 21, pp. 21204–21213, Nov. 2022, doi: 10.1109/JIOT.2022.3177581.

[23] F. Wang, F. Yang, C. Pan, J. Song, and Z. Han, “Joint Illumination and Communication Optimization in Indoor VLC for IoT Applications,” IEEE Internet of Things Journal, vol. 9, no. 21, pp. 20788–20800, Nov. 2022, doi: 10.1109/JIOT.2022.3175937.

[24] J. Kong, M. Ismail, E. Serpedin, and K. A. Qaraqe, “Energy Efficient Optimization of Base Station Intensities for Hybrid RF/VLC Networks,” IEEE Transactions on Wireless Communications, vol. 18, no. 8, pp. 4171–4183, Aug. 2019, doi: 10.1109/TWC.2019.2922611.

[25] M. S. Esfahani, A. M. Rahmani, M. Dehghan, and M. Reshadi, “Visible light communication networks MAC layer solutions: open issues and trends,” Photonic Network Communications, vol. 43, no. 2, pp. 116–134, Apr. 2022, doi: 10.1007/s11107-021-00954-8.

[26] Q. Hu, C. Gan, X. Liu, G. Gong, and Y. Zhu, “Dynamic handover cost modeling in hybrid VLC/RF networks,” Ad Hoc Networks, vol. 146, p. 103174, Jul. 2023, doi: 10.1016/j.adhoc.2023.103174.

[27] A. Zeshan and T. Baykas, “Location Aware Vertical Handover in a VLC/WLAN Hybrid Network,” IEEE Access, vol. 9, pp. 129810–129819, 2021, doi: 10.1109/ACCESS.2021.3113286.

[28] O. Narmanlioglu and M. Uysal, “Event-Triggered Adaptive Handover for Centralized Hybrid VLC/MMW Networks,” IEEE Transactions on Communications, vol. 70, no. 1, pp. 455–468, Jan. 2022, doi: 10.1109/TCOMM.2021.3120719.

[29] K. Küçük, D. L. Msongaleli, O. Akbulut, A. Kavak, and C. Bayılmış, “Self-adaptive medium access control protocol for aggregated VLC–RF wireless networks,” Optics Communications, vol. 488, p. 126837, Jun. 2021, doi: 10.1016/j.optcom.2021.126837.

[30] M. Amjad, H. K. Qureshi, S. A. Hassan, A. Ahmad, and S. Jangsher, “Optimization of MAC Frame Slots and Power in Hybrid VLC/RF Networks,” IEEE Access, vol. 8, pp. 21653–21664, 2020, doi: 10.1109/ACCESS.2020.2968624.

[31] M. Obeed, H. Dahrouj, A. M. Salhab, S. A. Zummo, and M.-S. Alouini, “User Pairing, Link Selection, and Power Allocation for Cooperative NOMA Hybrid VLC/RF Systems,” IEEE Transactions on Wireless Communications, vol. 20, no. 3, pp. 1785–1800, Mar. 2021, doi: 10.1109/TWC.2020.3036444.

[32] O. L. A. López et al., "Energy-Sustainable IoT Connectivity: Vision, Technological Enablers, Challenges, and Future Directions," in IEEE Open Journal of the Communications Society, vol. 4, pp. 2609-2666, 2023.

[33] S. Özyurt, A. F. Coşkun, S. Büyükçorak, G. Karabulut Kurt and O. Kucur, "A Survey on Multiuser SWIPT Communications for 5G+," in IEEE Access, vol. 10, pp. 109814-109849, 2022.

[34] D. I. Kim, J. H. Moon and J. J. Park, "New SWIPT using PAPR: How it works", IEEE Wireless Commun. Lett., vol. 5, no. 6, pp. 672-675, Dec. 2016.

[35] M. Rajabi, N. Pan, S. Claessens, S. Pollin and D. Schreurs, "Modulation techniques for simultaneous wireless information and power transfer with an integrated rectifier–receiver", IEEE Trans. Microw. Theory Techn., vol. 66, no. 5, pp. 2373-2385, May 2018.

[36] P. Dhull, D. Schreurs, G. Paolini, A. Costanzo, M. Abolhasan and N. Shariati, "Multitone PSK modulation design for simultaneous wireless information and power transfer", IEEE Trans. Microw. Theory Techn., vol. 72, no. 1, pp. 446-460, Jan. 2024.

[37] S. Claessens, N. Pan, D. Schreurs and S. Pollin, "Multitone FSK modulation for SWIPT", IEEE Trans. Microw. Theory Techn., vol. 67, no. 5, pp. 1665-1674, May 2019.

[38] N. Ayir, T. Riihonen and M. Heino, "Practical Waveform-to-Energy Harvesting Model and Transmit Waveform Optimization for RF Wireless Power Transfer Systems," in IEEE Transactions on Microwave Theory and Techniques, vol. 71, no. 12, pp. 5498-5514, Dec. 2023.

[39] G. Paolini et al., "RF Energy Harvesting from GFSK-Modulated BLE Signals," 2021 IEEE Topical Conference on Wireless Sensors and Sensor Networks (WiSNeT), San Diego, CA, USA, 2021, pp. 27-29.

[40] H. Ojukwu, B. -C. Seet and S. U. Rehman, "Metasurface-Aided Wireless Power Transfer and Energy Harvesting for Future Wireless Networks," in IEEE Access, vol. 10, pp. 52431-52450, 2022

[41] O. Alamu, T. O. Olwal and K. Djouani, ”Simultaneous lightwave information and power transfer in optical wireless communication networks: An overview and outlook,” Optik, vol. 266, 2022, 169590.

[42] K. Hammoud, M. Liu, Z. Cui, D. Schreurs and S. Pollin, "Enhanced Indoor Light Energy Harvesting Exploiting Over-The-Air Pulse Shaping," 2024 IEEE Wireless Power Technology Conference and Expo (WPTCE), Kyoto, Japan, 2024, pp. 477-481.

[43] H. Lim, Y. Park and Y. Song, "Underwater SLIPT Prototype System With a Combined Solar Panel-Photodiode Receiver: Design, Implementation, and Operation Strategy," in IEEE Wireless Communications Letters, vol. 13, no. 12, pp. 3673-3677, Dec. 2024.

[44] T. Tang, L. Shi, Q. Li and Z. Xiong, "Sustainability-Driven Resource Allocation for SLIPT-Assisted Hybrid VLC/RF IoT Systems," in IEEE Wireless Communications Letters, vol. 13, no. 6, pp. 1765-1769, June 2024

[45] Y. Xiao, P. D. Diamantoulakis, Z. Fang, L. Hao, Z. Ma and G. K. Karagiannidis, "Cooperative Hybrid VLC/RF Systems With SLIPT," in IEEE Transactions on Communications, vol. 69, no. 4, pp. 2532-2545, April 2021

[46] S. Sepehrvand, L. N. Theagarajan, and S. Hranilovic, “Rate-power trade- off in simultaneous lightwave information and power transfer systems,” IEEE Communications Letters, vol. 25, no. 4, pp. 1249–1253, 2021.

[47] I. Tavakkolnia, L. K. Jagadamma, R. Bian, P. P. Manousiadis, S. Videv, G. A. Turnbull, I. D. W. Samuel, and H. Haas, “Organic photovoltaics for simultaneous energy harvesting and high-speed MIMO optical wireless communications,” Light: Science & Applications, vol. 10, no. 41, 2021.

[48] T. Tang, T. Shang, Q. Li, G. Li, and B. Bai, “Energy-efficient subchannel assignment and power allocation in VLC-IoT systems with SLIPT,” Opt. Express, vol. 30, no. 22, pp. 39 492–39 509, Oct 2022.

[49] A. Tsiatmas, F. M. Willems, J.-P. M. Linnartz, S. Baggen, and J. W. Bergmans, “Joint illumination and visible-light communication systems: Data rates and extra power consumption,” 2015 IEEE International Conference on Communication Workshop (ICCW), pp. 1380–1386, 2015.

[50] C. Li, L. Mo, and D. Zhang, "Review on UHF RFID Localization Methods," IEEE Journal of Radio Frequency Identification, vol. 3, no. 4, pp. 205-215, Dec. 2019, doi: 10.1109/JRFID.2019.2924346.

[51] T. M. Schafer, J. Maurer, J. von Hagen, and W. Wiesbeck, “Experimental characterization of radio wave propagation in hospitals,” IEEE Transactions on Electromagnetic Compatibility, vol. 47, no. 2, pp. 304-311, May 2005, doi: 10.1109/TEMC.2005.847376.

[52] J. A. Flint, A. R. Ruddle, and A. E. May, “Coupling between Bluetooth modules inside a passenger car,” in Proc. International Conference on Antennas and Propagation, Exeter, UK, 2003, pp. 397-400, doi: 10.1049/cp:20030096.

[53] Y. Jia, M. Zhao, W. Zhou, and D. Peng, “Measurement and statistical analysis of 1.89GHz radio propagation in a realistic mountain tunnel,” in Proc. International Conference on Wireless Communications & Signal Processing, Nanjing, China, 2015, pp. 1-5, doi: 10.1109/WCSP.2015.7341050.

[54] M. V. S. Chandrashekhar, P. Choi, K. Maver, R. Sieber, and K. Pahlavan, “Evaluation of interference between IEEE 802.11b and Bluetooth in a typical office environment,” in Proc. IEEE International Symposium on Personal, Indoor and Mobile Radio Communications, San Diego, CA, USA, 2001, doi: 10.1109/PIMRC.2001.965494.

[55] S. Verma, A. Shandilya, and A. Singh, “A model for reducing the effect of ambient light source in VLC system,” in Proc. IEEE International Advance Computing Conference, Gurgaon, India, 2014, pp. 186-188, doi: 10.1109/IAdCC.2014.6779317.

[56] Y. Liu et al., “Reconfigurable Intelligent Surfaces: Principles and Opportunities,” in IEEE Communications Surveys & Tutorials, vol. 23, no. 3, pp. 1546-1577, thirdquarter 2021, doi: 0.1109/COMST.2021.3077737.

[57] Cisco, “Cisco visual networking index: Global mobile data traffic forecast update, 2017–2022”. White Paper, 2019.

[58] M. Kamel, W. Hamouda, and A. Youssef. “Ultra-dense networks: A survey,” IEEE Communications Surveys & Tutorials, 2016, doi: 10.1109/COMST.2016.2571730.

[59] Y. Murillo, “System Design and Characterization of Bluetooth Low Energy Mesh Networks,” PhD thesis, KU Leuven, Leuven, Belgium, 2020.

[60] Y. Murillo, A. Chiumento, B. Reynders, and S. Pollin, “An all-wireless SDN framework for BLE mesh,” ACM Transactions on Internet of Things, 2020, doi: 10.1145/3403581.

[61] T. Ylonen and C. Lonvick, “The secure shell (SSH) protocol architecture (No. rfc4251),” 2006.

[62] D. Law, D. Dove, J. D’Ambrosia, M. Hajduczenia, M. Laubach, and S. Carlson, “Evolution of ethernet standards in the IEEE 802.3 working group,” IEEE Communications Magazine, vol. 51, pp. 88–96, 2013, doi: 10.1109/MCOM.2013.6576344.

[63] B. Bellalta, “IEEE 802.11ax: High-efficiency WLANS,” IEEE Wireless Communications, vol. 23, pp. 38–46, 2 2016, doi: 10.1109/MWC.2016.7422404.

[64] Raspberry Corporation, “Raspberry Pi 4 model b specifications – raspberry pi,” available online (9.8.2023): https://www.raspberrypi.com/products/raspberry-pi-4-model-b/specifications/

[65] A. Galisteo, D. Juara, and D. Giustiniano, “Research in Visible Light Communication Systems with OpenVLC1.3,” in Proc. IEEE World Forum on Internet of Things, 2019, doi: 10.1109/WF-IoT.2019.8767252.

[66] S. Raza, P. Misra, Z. He, and T. Voigt, “Bluetooth smart: An enabling technology for the Internet of Things,” in Proc. IEEE 11th International Conference on Wireless and Mobile Computing, Networking and Communications, 2015, doi: 10.1109/WiMOB.2015.7347955.

[67] Nordic Semiconductor, “nrf52 dk,” available online (9.8.2023): https://www.nordicsemi.com/Products/Development-hardware/nrf52-dk

[68] C. Li, L. Mo, and D. Zhang, "Review on UHF RFID Localization Methods," IEEE Journal of Radio Frequency Identification, vol. 3, no. 4, pp. 205-215, Dec. 2019, doi: 10.1109/JRFID.2019.2924346.

[69] J. Luo, L. Fan, and H. Li, "Indoor Positioning Systems Based on Visible Light Communication: State of the Art," IEEE Communications Surveys & Tutorials, vol. 19, no. 4, pp. 2871-2893, Fourthquarter 2017, doi: 10.1109/COMST.2017.2743228.

[70] T. Sanpechuda and L. Kovavisaruch, "A review of RFID localization: Applications and techniques," in Proc. 5th International Conference on Electrical Engineering/Electronics, Computer, Telecommunications and Information Technology, Krabi, Thailand, 2008, pp. 769-772, doi: 10.1109/ECTICON.2008.4600544.

[71] P. V. Nikitin, R. Martinez, S. Ramamurthy, H. Leland, G. Spiess, and K. V. S. Rao, "Phase based spatial identification of UHF RFID tags," in Proc. IEEE International Conference on RFID, Orlando, FL, USA, 2010, pp. 102-109, doi: 10.1109/RFID.2010.5467253.

[72] J. Armstrong, Y. A. Sekercioglu, and A. Neild, "Visible light positioning: a roadmap for international standardization," IEEE Communications Magazine, vol. 51, no. 12, pp. 68-73, December 2013, doi: 10.1109/MCOM.2013.6685759.

[73] N. Chaudhary, L. N. Alves, and Z. Ghassemblooy, "Current Trends on Visible Light Positioning Techniques," in Proc. 2nd West Asian Colloquium on Optical Wireless Communications, Tehran, Iran, 2019, pp. 100-105, doi: 10.1109/WACOWC.2019.8770211.

[74] A. -C. Anastou, K. K. Delibasis, A. -A. A. Boulogeorgos, H. G. Sandalidis, A. Vavoulas, and S. K. Tasoulis, "A Low Complexity Indoor Visible Light Positioning Method," IEEE Access, vol. 9, pp. 57658-57673, 2021, doi: 10.1109/ACCESS.2021.3072348.

[75] J. Hightower, G. Borriello, and R. Want, "SpotON: An indoor 3D location sensing technology based on RF signal strength," Dept. Comput. Sci. Eng., Univ. Washington, Seattle, WA, USA, Rep. UWCSE00-02-02,2000.

[76] L. M. Ni, Yunhao Liu, Yiu Cho Lau, and A. P. Patil, "LANDMARC: indoor location sensing using active RFID," in Proc. 1st IEEE International Conference on Pervasive Computing and Communications, 2003, Fort Worth, TX, USA, 2003, pp. 407-415, doi: 10.1109/PERCOM.2003.1192765.

[77] W. Shi and V. W. S. Wong, "MDS-Based Localization Algorithm for RFID Systems," in Proc. IEEE International Conference on Communications, Kyoto, Japan, 2011, pp. 1-6, doi: 10.1109/icc.2011.5962800.

[78] F. Galler, S. Grebien, T. Faseth, K. Witrisal, G. Magerl, and H. Arthaber, "Extension of an SDR UHF RFID Testbed for MIMO and Monostatic Time of Flight Based Ranging," IEEE Journal of Radio Frequency Identification, vol. 1, no. 1, pp. 32-38, March 2017, doi: 10.1109/JRFID.2017.2749200.

[79] H. Arthaber, T. Faseth, and F. Galler, "Spread-Spectrum Based Ranging of Passive UHF EPC RFID Tags," IEEE Communications Letters, vol. 19, no. 10, pp. 1734-1737, Oct. 2015, doi: 10.1109/LCOMM.2015.2469664.

[80] Y. Ma, K. Pahlavan, and Y. Geng, "Comparative behavioral modeling of POA and TOA ranging for location-awareness using RFID," International Journal Wireless Information Networks, vol. 23, no. 3, pp. 187–198, 2016, doi: 10.1007/s10776-016-0311-6.

[81] X. Li, Y. Zhang, and M. G. Amin, "Multifrequency-based range estimation of RFID tags," in Proc. IEEE International Conference on RFID, 2009, pp. 147–154, doi: 10.1109/RFID.2009.4911199.

[82] A. Povalac and J. Sebesta, "Phase difference of arrival distance estimation for RFID tags in frequency domain," in Proc. IEEE International Conference on RFID Technology Applications, 2011, pp. 188–193, doi: 10.1109/RFID-TA.2011.6068636.

[83] J. Zhou, H. Zhang, and L. Mo, "Two-dimension localization of passive RFID tags using AOA estimation," in Proc. IEEE International Instrumentation and Measurement Technologies Conference, 2011, pp. 1–5, doi: 10.1109/IMTC.2011.5944170.

[84] S. Azzouzi, M. Cremer, U. Dettmar, R. Kronberger, and T. Knie, "New measurement results for the localization of UHF RFID transponders using an Angle of Arrival (AoA) approach," in Proc. IEEE International Conference on RFID, Orlando, FL, USA, 2011, pp. 91-97, doi: 10.1109/RFID.2011.5764607.

[85] P. Zand, J. Romme, J. Govers, F. Pasveer, and G. Dolmans, "A high-accuracy phase-based ranging solution with Bluetooth Low Energy (BLE)," in Proc. IEEE Wireless Communications and Networking Conference, Marrakesh, Morocco, 2019, pp. 1-8, doi: 10.1109/WCNC.2019.8885791.

[86] P. Boer, J. Romme, J. Govers, and G. Dolmans, "Performance of High-Accuracy Phase-Based Ranging in Multipath Environments," in Proc. IEEE 91st Vehicular Technology Conference, Antwerp, Belgium, 2020, pp. 1-5, doi: 10.1109/VTC2020-Spring48590.2020.9128721.

[87] E. L. Berz, D. A. Tesch, and F. P. Hessel, "RFID indoor localization based on support vector regression and k-means," in Proc. 24th IEEE International Symposium on Industrial Electronics, 2015, pp. 1418–1423, doi: 10.1109/ISIE.2015.7281681.

[88] Z. Belhadi and L. Fergani, "Fingerprinting methods for RFID tag indoor localization," in Proc. International Conference on Multimedia Computing and Systems, 2014, pp. 717–722, doi: 10.1109/ICMCS.2014.6911192.

[89] S. Bastiaens, "Towards centimetre-order indoor localisation with RSS-based visible light positioning," PhD thesis, Ghent University, Ghent, Belgium, 2022.

[90] J. A. Paradiso and T. Starner, "Energy scavenging for mobile and wireless electronics," IEEE Pervasive Computing, vol. 4, no. 1, pp. 18-27, Jan.-March 2005, doi: 10.1109/MPRV.2005.9.

[91] X. Lu, P. Wang, D. Niyato, D. I. Kim, and Z. Han, "Wireless Networks With RF Energy Harvesting: A Contemporary Survey," IEEE Communications Surveys & Tutorials, vol. 17, no. 2, pp. 757-789, doi: 10.1109/COMST.2014.2368999.

[92] Y. Alsaba, S. K. A. Rahim, and C. Y. Leow, “Beamforming in Wireless Energy Harvesting Communications Systems: A Survey,” IEEE Communications Surveys & Tutorials, vol. 20, no. 2, pp. 1329-1360, doi: 10.1109/COMST.2018.2797886.

[93] J. Hu, K. Yang, G. Wen, and L. Hanzo, “Integrated Data and Energy Communication Network: A Comprehensive Survey,” IEEE Communications Surveys & Tutorials, vol. 20, no. 4, pp. 3169-3219, Fourthquarter 2018, doi: 10.1109/COMST.2018.2860778.

[94] X. Lu, P. Wang, D. Niyato, D. I. Kim, and Z. Han, “Wireless Charging Technologies: Fundamentals, Standards, and Network Applications,” IEEE Communications Surveys & Tutorials, vol. 18, no. 2, pp. 1413-1452, doi: 10.1109/COMST.2015.2499783.

[95] H. Ojukwu, B. -C. Seet, and S. U. Rehman, “Metasurface-Aided Wireless Power Transfer and Energy Harvesting for Future Wireless Networks,” IEEE Access, vol. 10, pp. 52431-52450, 2022, doi: 10.1109/ACCESS.2022.3170106.

[96] V. Pecunia, et al.,”Roadmap on Energy Harvesting Materials. Journal of Physics,” Materials, vol. 6, no. 4, Aug. 2023, doi: 10.1088/2515-7639/acc550.

[97] J. Svarc, “Most Efficient Solar Panels 2023,” Clean Energy Review, available online (2.8.2023) https://www.cleanenergyreviews.info/blog/most-efficient-solar-panels

[98] J. Petäjäjärvi, J. Kaleva, K. Mikhaylov, H. Pulkkinen, J. Ahola, and M. Björkgren, “Automatic charging of an energy harvesting powered sensor node from controllable energy source,” in Proc. 14th International Wireless Communications and Mobile Computing Conference, Limassol, Cyprus, 2018, pp. 600-605, doi: 10.1109/IWCMC.2018.8450521.

[99] L. Summerer and O. Purcell, “Concepts for wireless energy transmission via laser,” in Proc. International Conference on Space Optical Systems and Applications, 2009.

[100] PowerLight, “How it works,” available online (2.8.2023): https://powerlighttech.com/how-it-works/

[101] Locheed Martin, “Lockheed Martin Performs First Ever Outdoor Flight Test Of Laser Powered UAS,” available online (2.8.2023): https://web.archive.org/web/20160723234624/http://www.lockheedmartin.com/us/news/press-releases/2012/august/120807ae_uas-laser-powered.html

[102] O. L. A. Lopez, et al., “Energy-Sustainable IoT Connectivity: Vision, Technological Enablers, Challenges, and Future Directions,” available online (2.8.2023): https://arxiv.org/abs/2306.02444

[103] Powercast, “Wireless Power/Charging,” available online (2.8.2023): https://www.powercastco.com/wireless-power/

[104] S. Roy, J. -J. Tiang, M. B. Roslee, M. T. Ahmed, and M. A. P. Mahmud, “A Quad-Band Stacked Hybrid Ambient RF-Solar Energy Harvester With Higher RF-to-DC Rectification Efficiency,” IEEE Access, vol. 9, pp. 39303-39321, 2021, doi: 10.1109/ACCESS.2021.3064348.

[105] A. H. F. Raouf, C. K. Anjinappa, and I. Guvenc, “Optimal Design of Energy-Harvesting Hybrid VLC/RF Networks,” in Proc. IEEE Globecom Workshops, Rio de Janeiro, Brazil, 2022, pp. 705-710, doi: 10.1109/GCWkshps56602.2022.10008721.

[106] S. Zargari, M. Kolivand, S. A. Nezamalhosseini, B. Abolhassani, L. R. Chen, and M. H. Kahaei, “Resource Allocation of Hybrid VLC/RF Systems With Light Energy Harvesting,” IEEE Transactions on Green Communications and Networking, vol. 6, no. 1, pp. 600-612, March 2022, doi: 10.1109/TGCN.2021.3097051.

[107] Y. Yapıcı and İ. Güvenç, “Energy- vs Spectral-Efficiency for Energy-Harvesting Hybrid RF/VLC Networks,” in Proc. 54th Asilomar Conference on Signals, Systems, and Computers, Pacific Grove, CA, USA, 2020, pp. 1152-1156, doi: 10.1109/IEEECONF51394.2020.9443343.

[108] Powercast Corporation, “PCC110 RF-to-DC Converter Chip User Manual”, available online (13.12.24): https://www.powercastco.com/wp-content/uploads/2024/11/New-PCC110-Datasheet.pdf

[109] S. Geysen, “Design and implementation of a Bluetooth Low Energy NS-3 module for simulation of large Bluetooth Low Energy mesh networks,” KU Leuven, 2018.

[110] A. Aldalbahi et al., “Extending ns3 to simulate visible light communication at network-level,” in 2016 23rd International Conference on Telecommunications (ICT), 2016, pp. 1–6. doi: 10.1109/ICT.2016.7500485.

[111] A. Aldalbahi, M. Rahaim, A. Khreishah, M. Ayyash, and T. D. C. Little, "Visible Light Communication Module: An Open Source Extension to the ns3 Network Simulator With Real System Validation," IEEE Access, vol. 5, pp. 22144–22158, 2017, doi: 10.1109/ACCESS.2017.2759779.

[112] ns-3 Documentation – Energy Model API Architecture and API. The ns-3 Project, 2018, available online (1.5.2023): https://www.nsnam.org/wiki/Energy_model

[113] M. Capuzzo, C. Delgado, J. Famaey, and A. Zanella, "An Ns-3 Implementation of a Battery-Less Node for Energy-Harvesting Internet of Things," in Proceedings of the 2021 Workshop on Ns-3, 2021, pp. 57–64. doi: 10.1145/3460797.3460805.

[114] Ö. Bulakci and Xi Li, "6G Architecture WG – On the Way to 6G," 6GSNS presentation at EuCNC'24, available online (10.12.2024): https://hexa-x-ii.eu/wp-content/uploads/2024/06/01-SNS-JU-6G-Arch-WG_EuCNC2024_PDF.pdf

[115] M. Uusitalo et al. (Eds.) "European Vision for the 6G Network Ecosystem," available online (10.12.2024): https://doi.org/10.5281/zenodo.14230482

[116] Ö. Bulakci, et al. (Eds.) "Towards Sustainable and Trustworthy 6G: Challenges, Enablers, and Architectural Design," now Publishers Inc., 2023.

[117] 3GPP, "5G System Overview," available online (10.12.2024): https://www.3gpp.org/technologies/5g-system-overview

[118] Bluetooth SIG, "Bluetooth Core Specification," version 5.4, 31.1.2023.

[119] Nordic Semiconductors, "nRF52 DK," available online (10.8.2023): https://www.nordicsemi.com/Products/Development-hardware/nrf52-dk

[120] Nordic Semiconductors, "Radio Test Example," available online (10.8.2023): https://infocenter.nordicsemi.com/index.jsp?topic=%2Fcom.nordic.infocenter.sdk5.v11.0.0%2Fnrf_radio_test_example.html

[121] Xiong Deng, Yan Wu, A. M. Khalid, Xi Long, and Jean-Paul M. G. Linnartz, "LED power consumption in joint illumination and communication system," Opt. Express 25, 18990-19003 (2017).

11 List of Figures

12 List of Tables

13 List of contributors

Contributors	**Short name**	**Country**
OULUN YLIOPISTO	UOULU	Finland
STICHTING IMEC NEDERLAND	IMEC-NL	Netherlands
KATHOLIEKE UNIVERSITEIT LEUVEN	KU Leuven	Belgium
INSTITUTO DE ENGENHARIA DE SISTEMAS E COMPUTADORES, TECNOLOGIA E CIÊNCIA	INESC TEC	Portugal
UNIVERSITY OF BRISTOL	U of Bristol	United Kingdom

14 Appendix 1: List of scenarios and applications identified in SUPERIOT D1.1 version 1.0

SUPERIOT-SCN-1: smart tags and labels

- SUPERIOT Application 1.1 - Smart labels attached or incorporated in day-to-day market products
- SUPERIOT Application 1.2 - Smart tags incorporated in sensitive items (high-value, high-risk, among others)
- SUPERIOT Application 1.3 - Tags and labels specifically designed for food and medicines
- SUPERIOT Application 1.4 - Labels specifically designed for logistic operations
- SUPERIOT Application 1.5 - Enhanced labels for batch manufacturing
- SUPERIOT Application 1.6 - Tags incorporated in shelves or in other small product packages
- SUPERIOT Application 1.7 - Tags and labels for healthcare patients
- SUPERIOT Application 1.8 - Tags for smart pills
- SUPERIOT Applications 1.9 - Labels for tracking critical equipment
- SUPERIOT Applications 1.10 - Tags for animal monitoring and management (livestock and wildlife)
- SUPERIOT Application 1.11 - Tags to increase collectible cards gaming experience

SUPERIOT-SCN-2: large-scale sensing and actuation

- SUPERIOT Application 2.1 - Sensors and actuators for smart buildings
- SUPERIOT Application 2.2 - Sensors and actuators for construction monitoring
- SUPERIOT Application 2.3 - Sensors for medical and safety applications
- SUPERIOT Application 2.4 - Sensors and actuators applied to smart cities
- SUPERIOT Application 2.5 - Sensors and actuators applied to smart agriculture and forestry

SUPERIOT-SCN-3: enhanced IoT communication in demanding environments

- SUPERIOT Application 3.1 - Secure and private IoT communication
- SUPERIOT Application 3.2 - Reliable IoT communication
- SUPERIOT Application 3.3 - Underwater IoT communication
- SUPERIOT Application 3.4 - In-body and on-body communication
- SUPERIOT Application 3.5 - Coverage extension with large-area IoT nodes
- SUPERIOT Application 3.6 - Resource extraction supported by IoT communication
- SUPERIOT Application 3.7 - Intelligent transportation systems
- SUPERIOT Application 3.8 - Sensorization and IoT communication in remote zones